International Journal of Astronomy and Astrophysics, 2016, 6, 464-493
http://www.scirp.org/journal/ijaa
ISSN Online: 2161-4725
ISSN Print: 2161-4717

Analysis of Effect of Solar Radiation Pressure of Bigger Primary on the Evolution of Periodic Orbits

Niraj Pathak[1], V. O. Thomas[2]

[1]Department of Mathematics, Dharmsinh Desai University, Nadiad, India
[2]Department of Mathematics, The Maharaja Sayajirao University of Baroda, Vadodara, India
Email: niraj23481@yahoo.com, votmsu@gmail.com

How to cite this paper: Pathak, N. and Thomas, V.O. (2016) Analysis of Effect of Solar Radiation Pressure of Bigger Primary on the Evolution of Periodic Orbits. *International Journal of Astronomy and Astrophysics*, **6**, 464-493.
http://dx.doi.org/10.4236/ijaa.2016.64037

Received: October 18, 2016
Accepted: December 24, 2016
Published: December 27, 2016

Abstract

Evolution of periodic orbits in Sun-Mars and Sun-Earth systems are analyzed using Poincare surface of section technique and the effects of solar radiation pressure of bigger primary and actual oblateness of smaller primary on these orbits are considered. It is observed that solar radiation pressure of bigger primary has substantial effect on period, orbit's shape, size and their position in the phase space. Since these orbits can be used for the design of low energy transfer trajectories, so perturbations due to solar radiation pressure has to be understood and should be taken care of during trajectory design. It is also verified that stability of such orbits are negligible so they can be used as transfer orbit. For each pair of solar radiation pressure q and Jacobi constant C we get two separatrices where stability of island becomes zero. In this paper, detailed stability analysis of periodic orbit having two loops is given when $q = 0.9845$.

Keywords

Restricted Three Body Problem, Low Energy Trajectory Design, Periodic Orbits, Solar Radiation Pressure, Poincare Surface of Section

1. Introduction

A Hohmann transfer (Hohmann, 1925) is effectively used to transfer a spacecraft from one circular orbit to another in a most fuel efficient way. The "low-energy" transfer trajectory [1] is used to describe the space trajectories that consume less fuel compared to Hohman transfer (Hohmann, 1925). The planar restricted three body problem (PRTBP) has long been used in celestial mechanics because it is one of the simplest non-integrable dynamic systems. RTBP refers to the motion of body of negligible mass, known as secondary body, under the sole influence of two massive primary bodies Sun-Earth, Earth-

Moon etc. For mathematical simplicity, we shall take the total mass of primaries normalized to 1. The mass of smaller primary is taken as μ so that the mass of its bigger counterpart is $1 - \mu$. The primaries are moving in a circular orbit in counter clockwise direction about their common center of mass with angular velocity normalized to 1. The third body, an artificial satellite or spacecraft, is moving in the same plane of motion of the primaries.

The "low-energy" transfer orbits are important in the study of practical problems regarding transfer of orbits. Low energy transfer of orbit to moon has been studied by [1]. In their study, they have considered four bodies Sun-Earth-Moon-Space craft as coupled three body systems, namely Sun-Earth-space craft and Earth-Moon-space craft. They constructed low energy transfer trajectories from the earth which executed capture at the Moon.

Study of orbits of bodies in RTBP has been described in detail by [2]. The equations of motion consist of non-linear equations and hence analytic methods seldom give physically useful results. So, a widely used method for describing the motion of secondary body (space craft) is the Poincare Surface of Section (PSS) method. [3] has given a detailed analysis of periodic orbits using PSS technique.

As per Kolmogorov-Arnold-Moser (KAM) theory (Moser, 1966), a fixed point on the Poincare surface of section represents a periodic orbit in the rotating frame, and the closed curves around the point correspond to the quasi-periodic orbits. [4] analyzed the PSS for Earth-Moon system without considering any perturbation. [5] also had analysed Sun-Mars system by incorporating perturbations due to solar radiation. They have identified periodic, quasi-periodic solutions and chaotic regions from the PSS. Similar studies have been made by [6] for Saturn Titan system. [7] analyzed the family "f" orbits around smaller primary under RTBP for 14 systems under ideal conditions. Recently, [8] analyzed Sun and Saturn centered periodic orbits with solar radiation pressure and oblateness and found that there is a substantial effect of solar radiation pressure on position and geometry of infinitesimal particle orbit. [9] had studied family "f" orbits and their stability for Sun-Saturn system with perturbation. In their study Sun was taken as a source of radiation and Saturn was considered as oblate spheroid. By taking the actual coefficient of oblateness for Saturn and different values of solar radiation pressure, the family "f" orbits has been analyzed in detail.

Periodic orbits of spacecraft around the two massive primaries are used to construct low energy trajectory. In this paper, we have studied periodic orbits around both primaries in the frame work of RTBP using PSS method. [10] established three classes with orbits around both primaries depending on motion of spacecraft is prograde or retrograde in the rotating system as well as fixed system. In this paper we have analyzed periodic orbits around both primaries with retrograde motion in rotating system and analyzed periodic orbits having number of loops from 1 to 5 for different pairs of solar radiation pressure q and Jacobi constant C for Sun-Mars and Sun-Earth system. It has been found that q and C have substantial effect on the position in phase space, shape and size of the orbits and hence must be considered during low energy trajectory design.

2. Equations of Motion

Let m_1 and m_2 be two masses of first and second primary bodies, respectively. Mass of first primary is greater than mass of second primary. The solar radiation pressure force F_p changes with the distance by the same law as the gravitational attraction force F_g and acts opposite to it. It is possible to consider that the result of the action of this force leads to reducing the effective mass of the sun [5]. Accordingly, the sun's resultant force acting on the particle is

$$F = F_g - F_p = F_g\left(1 - \frac{F_p}{F_g}\right) = qF_g, \tag{1}$$

where $q = 1 - \frac{F_p}{F_g}$, known as the mass reduction factor constant for the given particle. We follow the notation and terminology of [2]. It is clear from Equation (1) that $q = 1$ indicates $F = F_g$ and hence the solar radiation pressure drops to zero.

The perturbed mean motion n of second primary body is given by,

$$n^2 = 1 + \frac{3}{2}A_2 \tag{2}$$

where

$$A_2 = \frac{\rho_e^2 - \rho_p^2}{5R^2}. \tag{3}$$

Here A_2 is oblateness coefficient of second primary. ρ_e and ρ_p represent equatorial and polar radii of second primary and R is the distance between two primaries.

The unit of mass is chosen equal to the sum of the primary masses and the unit of length is equal to their separation. The unit of time is such that the Gaussian constant of gravitation is unity in the unperturbed case. The usual dimensionless synodic coordinate system Oxy is used to express the motion of the secondary body (space craft).

Choose a rotating coordinate system with origin at the center of mass, the primaries lie on the x-axis at the points $(-\mu, 0)$ and $(1 - \mu, 0)$, respectively, where mass factor $\mu = \frac{m_2}{(m_1 + m_2)}$. Following [11], the equations of motion of the spacecraft are

$$\ddot{x} - 2n\dot{y} = \frac{\partial\Omega}{\partial x}, \quad \ddot{y} + 2n\dot{x} = \frac{\partial\Omega}{\partial y}, \tag{4}$$

where

$$\Omega = \frac{n^2}{2}\left[(1-\mu)r_1^2 + \mu r_2^2\right] + \frac{q(1-\mu)}{r_1} + \frac{\mu}{r_2} + \frac{\mu A_2}{2r_2^3}. \tag{5}$$

Here

$$r_1^2 = (x - \mu)^2 + y^2, \tag{6}$$

and

$$r_2^2 = (x + 1 - \mu)^2 + y^2. \tag{7}$$

System of Equation (4) lead to the first integral

$$\dot{x}^2 + \dot{y}^2 = 2\Omega - C, \tag{8}$$

where C is Jacobi constant of integration given by

$$C = n^2\left[(1-\mu)r_1^2 + \mu r_2^2\right] + 2\frac{q(1-\mu)}{r_1} + 2\frac{\mu}{r_2} + \frac{\mu A_2}{r_2^3} - \dot{y}^2. \tag{9}$$

These equations of motion are integrated in (x, y) variables using a Runge-Kutta Gill fourth order variable or fixed step-size integrator. The initial conditions are selected along the x-axis. By defining a plane, say $y = 0$, in the resulting three dimensional space the values of x and $\dot{x}$ can be plotted every time the particle has $y = 0$, whenever the trajectory intersects the plane in a particular direction, say $\dot{y} > 0$. We have constructed Poincare surface section (PSS) on the x, $\dot{x}$ plane. The initial values were selected along the Ox-axis by using intervals of length 0.001. By giving different value of C we can plot the trajectories, and then analysis of orbits can be done.

3. Results and Discussion

We shall consider two systems, the Sun-Mars system and the Sun-Earth system. The masses of Sun, Earth and Mars are taken as 1.9881×10^{30} kg, 5.972×10^{24} kg, and 6.4185×10^{23} kg, respectively [5]. The mass factor μ, for the Sun-Earth and Sun-Mars systems, are 0.000003002 and 0.0000003212, respectively. Equatorial and polar radii of Earth are 6378.1 kms. and 6356.8 kms. and that of Mars are 3396.2 kms. and 3376.2 kms., respectively. The distance between Sun and Earth is taken as 149,600,000 kms. and distance between Sun and Mars is 227,940,000 kms. So, oblateness coefficient calculated from Equation (2) for Sun-Earth and Sun-Mars have values $A_2 = 2.42405 \times 10^{-12}$ and $A_2 = 5.21389 \times 10^{-13}$ respectively. $q = 1$ means that there is no perturbation due to solar radiation pressure and $q < 1$ indicates that we are including perturbation due to solar radiation pressure. For a given q, selection of C is not arbitrary. By solving Equation (9) w.r.t. $\dot{x}^2$ and by setting in to this equation $y = 0$ and $\dot{y}^2 > 0$ the resulting inequality defines the regions allowed to motion on the PSSs. Thus, we eliminate the possibility of excluded region for secondary body between Sun and Earth (or Mars). This maximum value of C is considered as admissible value of C.

Table 1 and Table 2 shows range of admissible values of C for Sun-Earth and Sun-Mars system. It can be observed that for Sun-Mars system size of excluded region is more than size of excluded region of Sun-Earth system. So, we can say that as mass factor increases, size of excluded region decreases. We have analyzed the effect of solar radiation pressure on admissible value of Jacobi constant C. We have studied the effect of solar radiation pressure on the location and period of Sun-Mars system for different values of Jacobi constant C using PSS. Figure 1 displays the PSS for Sun-Mars system for the pair (q, C) as (0.9845, 2.94) by taking value of x from the interval [0.8, 1] with interval of x differencing for x as 0.001. Also, time span t = 10,000 time units and interval of differencing for time is taken as 0.001. So, for each x equations of motions are

Table 1. Admissible range of C for Sun-Earth system.

q	Maximum value of C	Value of C greater than maximum value	Excluded region (where y is complex)	Size of excluded region
1	3.0	3.001	$x = 0.988$ to $x = 0.994$	0.006
0.995	2.99	2.991	x = 0.985 to x = 0.994	0.009
0.99	2.98	2.981	x = 0.983 to x = 0.995	0.012
0.9845	2.969	2.970	x = 0.98 to x = 0.995	0.015

Table 2. Admissible range of C for Sun-Mars system.

q	Maximum value of C	Value of C greater than maximum value	Excluded region (where y is complex)	Size of excluded region
1	3.0	3.001	$x = 0.984$ to $x = 1.0$	0.016
0.995	2.99	2.991	x = 0.982 to x = 1.0	0.018
0.99	2.98	2.981	x = 0.980 to x = 1.0	0.020
0.9845	2.969	2.970	x = 0.978 to x = 0.995	0.022

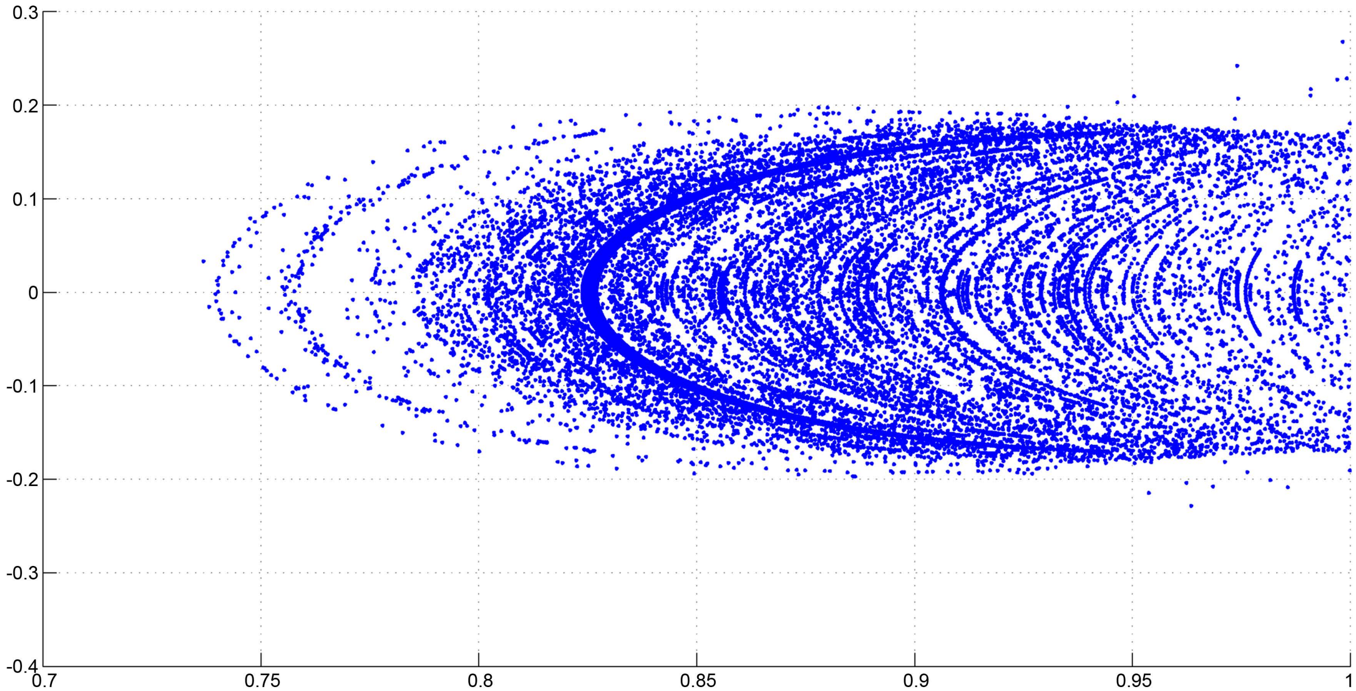

Figure 1. PSS for $q = 0.9845$ and $C = 2.94$, for $x = [0.8, 1]$, $t = 10{,}000$ for Sun-Mars system.

integrated using Runge-Kutta-Gill method. Each solution is plotted as a point in the $x - \dot{x}$ -plane in Figure 1. The arcs of PSS are known as islands whose center gives periodic orbits.

In a similar way, we have obtained PSS for Sun-Earth system as shown in Figure 2. This PSS is also constructed for the pair (q, C) given by (0.9845, 2.94). Our aim is to make a comparative study of the effect of solar radiation pressure on different parameters of the orbits of the secondary body (space craft) in the Sun-Earth and Sun-Mars systems using PSS technique. Mass factor μ of Sun-Earth is greater than Sun-Mars.

The numerical values of location and period of periodic orbit of spacecraft for C = 2.93, 2.94, 2.95, 2.96 and for q = 1, 0.995, 0.99 and 0.9845 are displayed in Table 3. It is

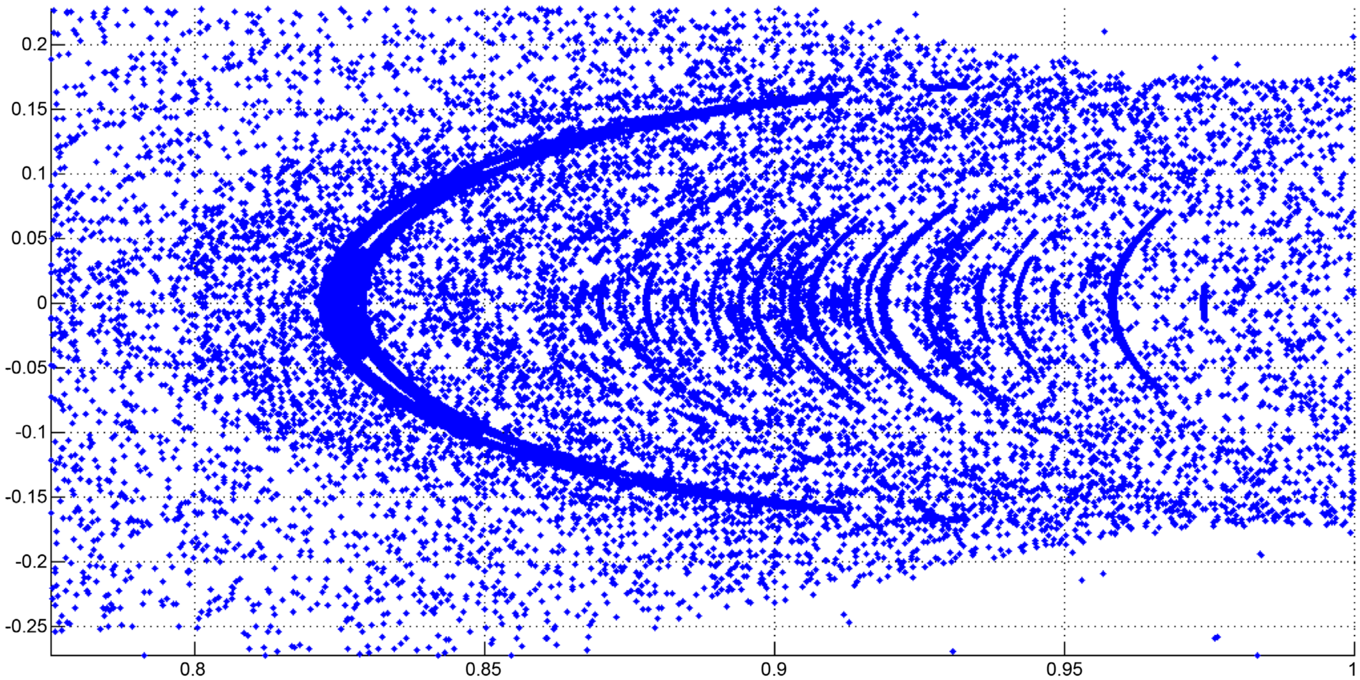

Figure 2. PSS for $q = 0.9845$ and $C = 2.94$, for $x = [0.8, 1]$, $t = 10{,}000$ for Sun-Earth system.

Table 3. Analysis of periodic orbit for different pairs of q and C for Sun-Mars system.

Number of loops	C	$q = 1$		$q = 0.995$		$q = 0.99$		$q = 0.9845$	
		Location (x)	Period (T)	Location (x)	Period (T)	Location (x)	Period (T)	Location (x)	Period (T)
1	2.96	0.983	13	0.9967	13	-	-	-	-
	2.95	0.96791	13	0.98115	13	0.9949	13	-	-
	2.94	0.95327	13	0.96607	13	0.97935	13	0.99455	13
	2.93	0.939	13	0.95139	13	0.96424	13	0.97891	13
2	2.96	0.94152	19	0.95985	19	0.97957	19	-	-
	2.95	0.92255	19	0.93971	19	0.95807	19	0.97992	19
	2.94	0.90454	19	0.92071	19	0.93792	19	0.95825	19
	2.93	0.88737	19	0.90269	19	0.91891	19	0.93795	19
3	2.96	0.91532	26	0.9363	26	0.95957	26	0.98875	26
	2.95	0.89429	26	0.91353	26	0.93455	26	0.96036	26
	2.94	0.87465	26	0.89248	26	0.91175	26	0.93506	26
	2.93	0.85619	26	0.87283	26	0.89069	26	0.91204	26
4	2.96	0.89707	32	0.91959	32	0.9451	32	0.9783	32
	2.95	0.87494	32	0.89529	32	0.91785	32	0.9462	32
	2.94	0.8545	32	0.87314	32	0.89353	32	0.91857	32
	2.93	0.835433	32	0.852695	32	0.871375	32	0.89397	32
5	2.96	0.883675	38	0.90711	38	0.93405	38	0.9701	38
	2.95	0.86093	38	0.8819	38	0.90538	38	0.93535	38
	2.94	0.84007	38	0.85915	38	0.88016	38	0.90623	38
	2.93	0.820715	38	0.83829	38	0.8574	38	0.88069	38

observed from the table that a change in C in the range (2.93, 2.96) affects the location but has no effect on the period and number of loops of the orbit. Solar radiation pressure also affects the location and period of the orbit. Similarly, the effects of C and q in the location and period for the Sun-Earth system are studied and the numerical estimates of the changes are displayed in Table 4. It can be seen that, for both the systems, the period of orbit increases with increase in the number of loops.

A noticeable difference observed in both the systems is that for $C = 2.96$, $q = 0.995$, single-loop periodic orbit, for $C = 2.96$, $q = 0.99$ two loops orbit, for $C = 2.96$, $q = 0.9845$, three loops periodic orbit does not exist for Sun-Earth system where as it exists for Sun-Mars system.

The periodic orbits starting from single-loop to five loops in the Sun-Mars system for $q = 0.9845$ and 0.995 are shown in Figures 3(a)-(j). It can be observed, from Figure 3 and Figure 4, that the width of the orbit decreases continuously as the number of loops increases. Also, as perturbation due to solar radiation pressure decreases from $q =$ 0.9845 to 0.995 we can observe that size of the loop increases. Further, it can be noticed that as the perturbation due to solar radiation pressure increases (that is, q decreases), the location of the closest approach of the space craft shifts towards the second primary body in both Sun-Mars and Sun-Earth system. This is contrary to the effect of oblateness of the second primary. That is, as the oblateness coefficient increases the position of the

Table 4. Analysis of periodic orbit for different pairs of q and C for Sun-Earth system.

Number of loops	C	$q = 1$		$q = 0.995$		$q = 0.99$		$q = 0.9845$	
		Location (x)	Period (T)	Location (x)	Period (T)	Location (x)	Period (T)	Location (x)	Period (T)
1	2.96	0.98305	13	-	-	-	-	-	-
	2.95	0.96795	13	0.9812	13	0.9949603	13	-	-
	2.94	0.9533	13	0.9661	13	0.9794	13	0.994601	13
	2.93	0.93904	13	0.95142	13	0.96425	13	0.97895	13
2	2.96	0.94157	19	0.9599	19	-	-	-	-
	2.95	0.92259	19	0.93975	19	0.95813	19	0.98	19
	2.94	0.90456	19	0.92075	19	0.93796	19	0.9583	19
	2.93	0.8874	19	0.90273	19	0.91895	19	0.938	19
3	2.96	0.91538	26	0.93635	26	0.95965	26	-	-
	2.95	0.89434	26	0.91359	26	0.93462	26	0.96045	26
	2.94	0.87469	26	0.89252	26	0.91181	26	0.93513	26
	2.93	0.85623	26	0.87287	26	0.89074	26	0.9121	26
4	2.96	0.89714	32	0.91965	32	0.9452	32	0.97844	32
	2.95	0.87499	32	0.89535	32	0.91793	32	0.9463	32
	2.94	0.85454	32	0.8732	32	0.89359	32	0.91865	32
	2.93	0.83547	32	0.85274	32	0.87142	32	0.89403	32
5	2.96	0.88373	38	0.90719	38	0.93415	38	0.9703	38
	2.95	0.86099	38	0.88195	38	0.90546	38	0.93547	38
	2.94	0.84012	38	0.8592	38	0.88022	38	0.9063	38
	2.93	0.82075	38	0.83833	38	0.85745	38	0.88075	38

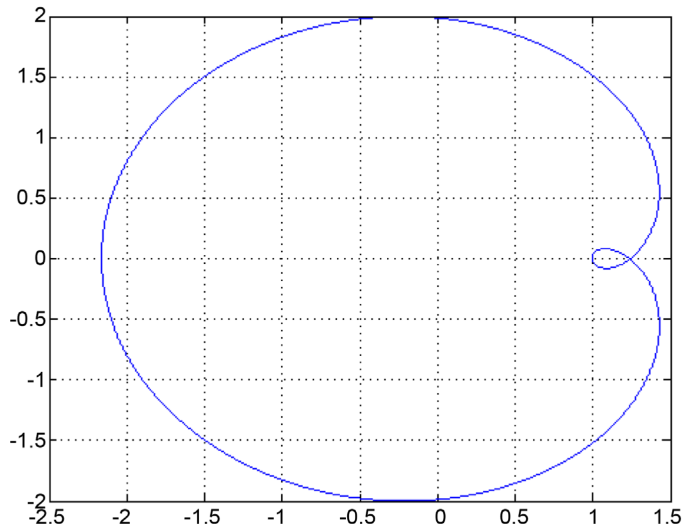

(a) $q = 0.9845$, single loop periodic orbit.

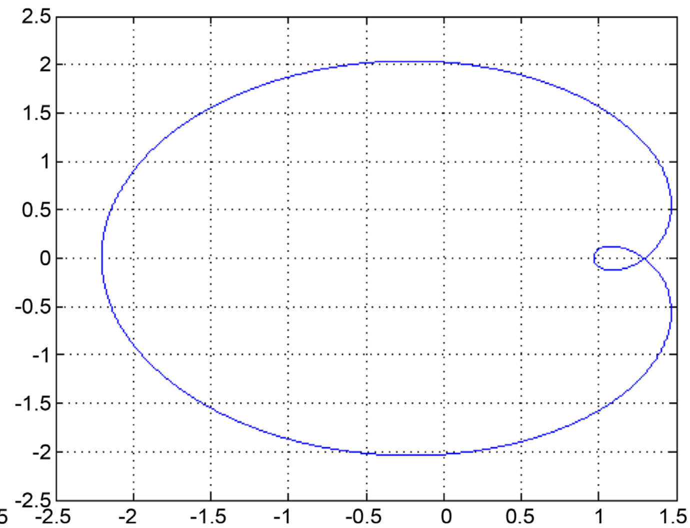

(b) $q = 0.995$, single loop periodic orbit.

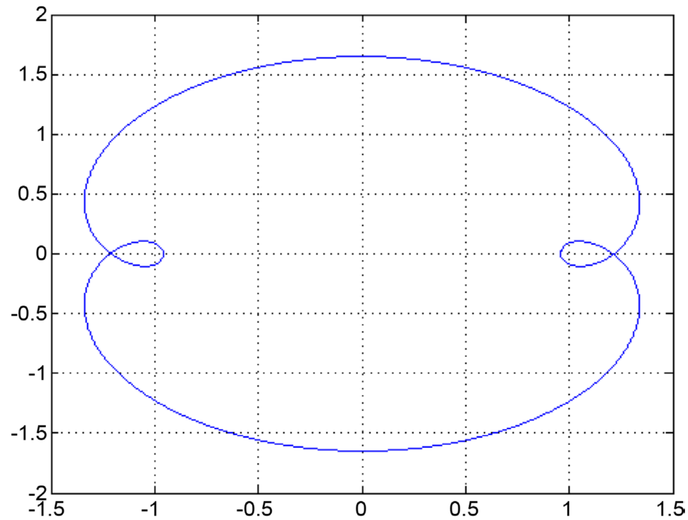

(c) $q = 0.9845$, two loops periodic orbit.

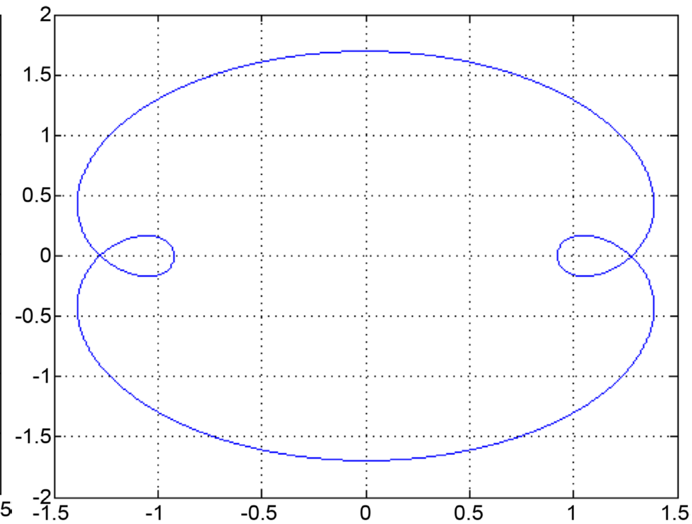

(d) $q = 0.995$, two loops periodic orbit.

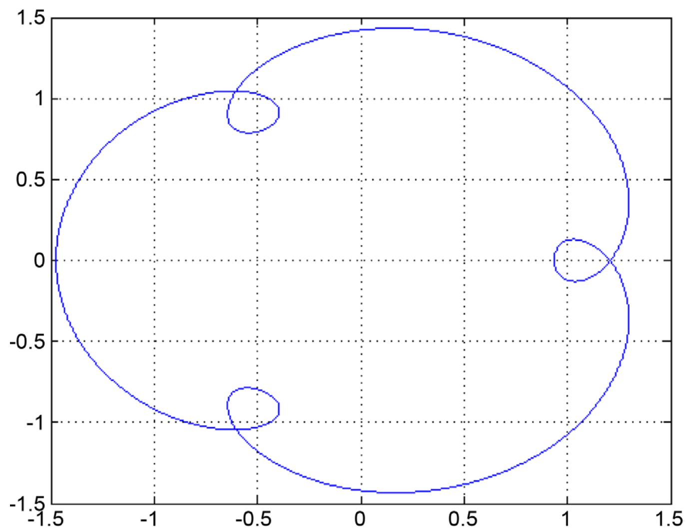

(e) $q = 0.9845$, three loops periodic orbit.

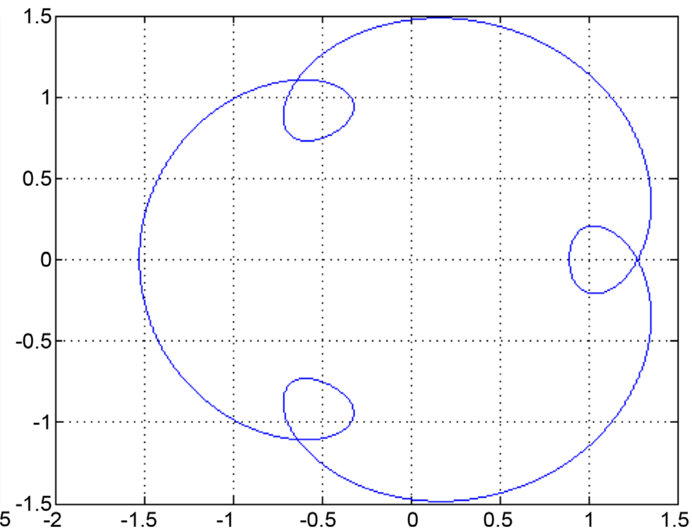

(f) $q = 0.995$, three loops periodic orbit.

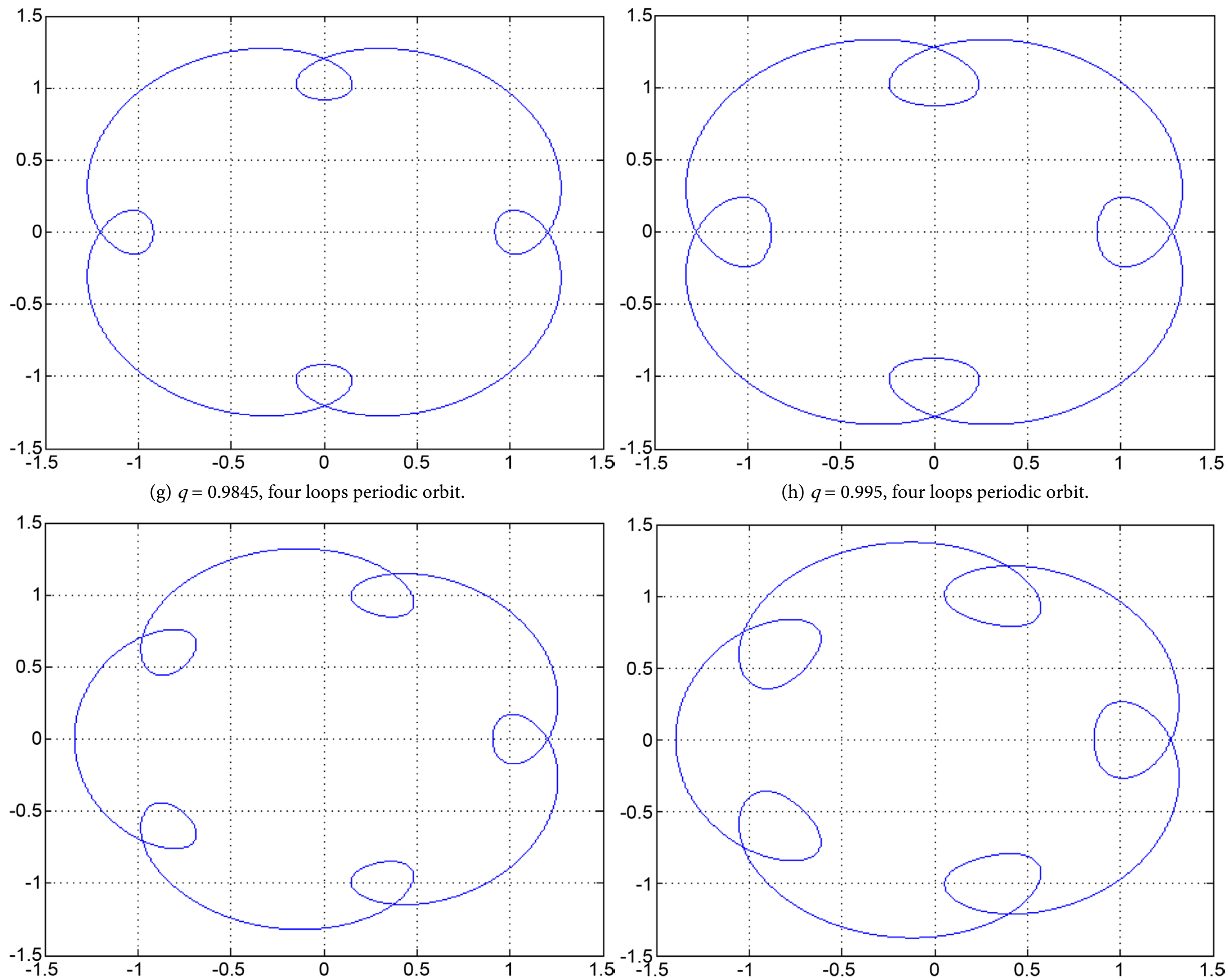

(g) $q = 0.9845$, four loops periodic orbit.

(h) $q = 0.995$, four loops periodic orbit.

(i) $q = 0.9845$, five loops periodic orbit.

(j) $q = 0.995$, five loops periodic orbit.

Figure 3. Periodic orbits around both primaries for Sun-Mars system for $C = 2.94$.

closest approach of the space craft receeds from the second primary [9]. Further in all cases the infinitesimal particle (space craft) orbits around the second primary (Mars) in addition to orbiting both primaries. Further the secondary body is closest to Mars in the single loop closed orbit. Such orbits may be useful in the study of different aspects of both primaries. In many models available in literature not many closed orbits possess this kind of nature. We can observe similar nature in the orbits shown in **Figures 4(a)-(j)** in the case of Sun-Earth system.

Figure 3 and **Figure 4** depict periodic orbits with number of loops varying from 1 to 5 with different solar radiation pressure for Sun-Mars and Sun-Earth systems, respectively. For both of these figures value of Jacobi constant C is 2.94. The expression for semi-major axis a and eccentricity e of the periodic orbits around both primaries are given by [3].

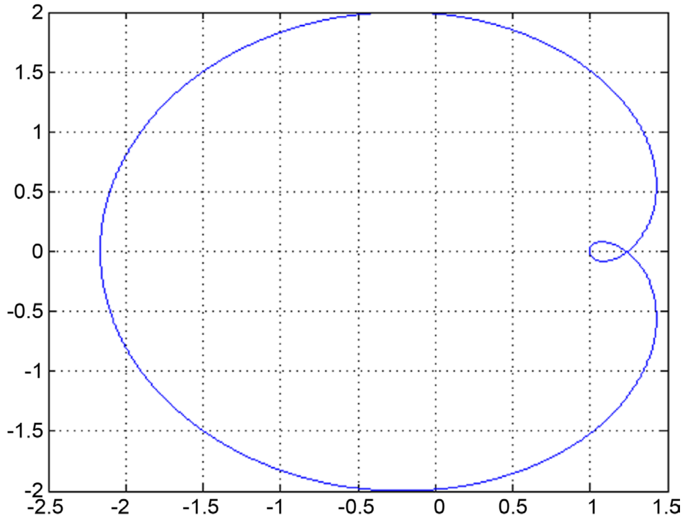

(a) $q = 0.9845$, single loop periodic orbit.

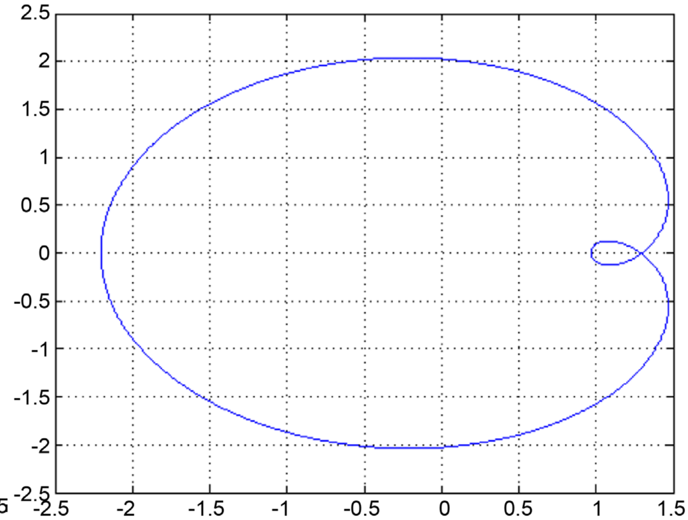

(b) $q = 0.995$, single loop periodic orbit.

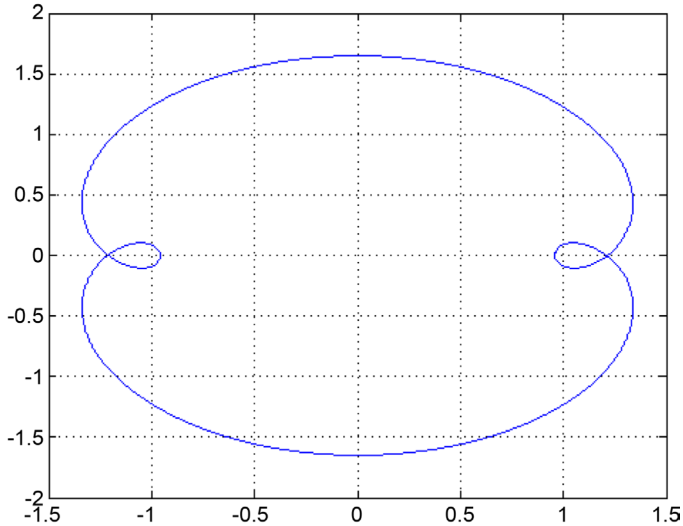

(c) $q = 0.9845$, two loops periodic orbit.

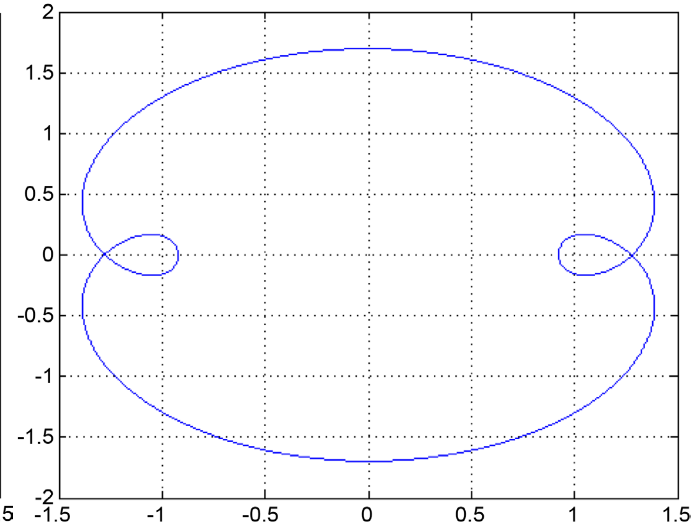

(d) $q = 0.995$, two loops periodic orbit.

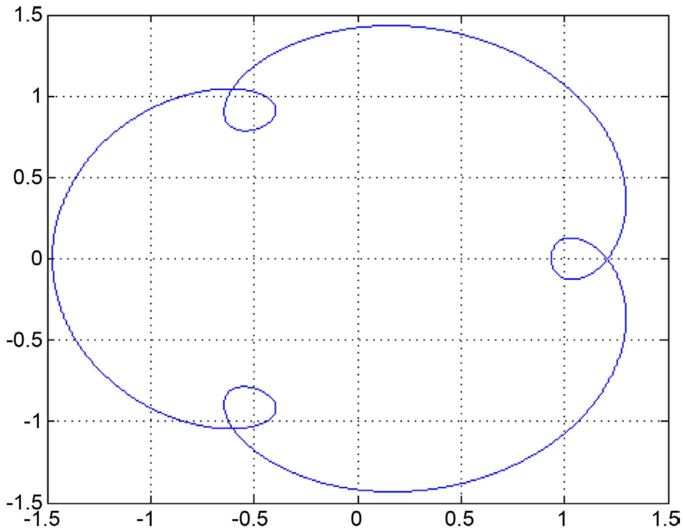

(e) $q = 0.9845$, three loops periodic orbit.

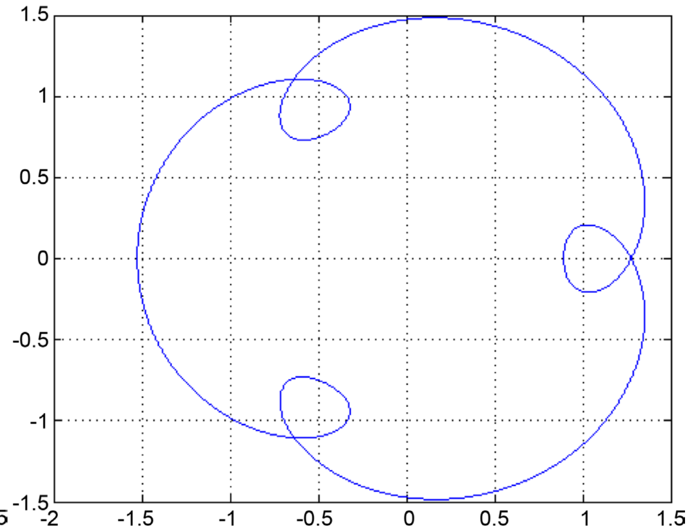

(f) $q = 0.995$, three loops periodic orbit.

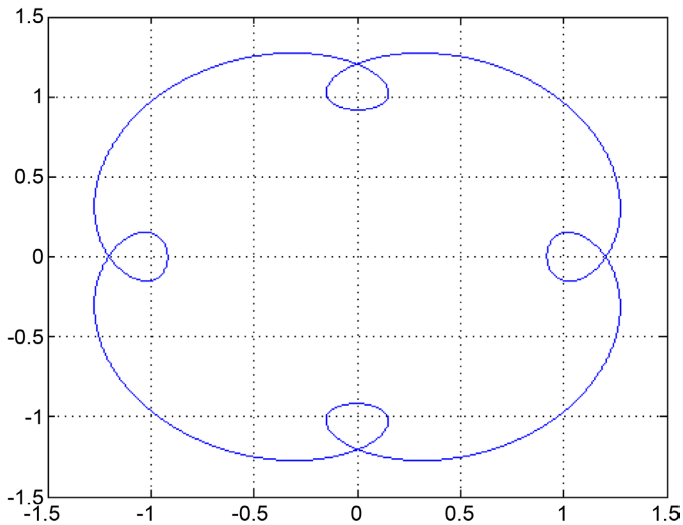

(g) $q = 0.9845$, four loops periodic orbit.

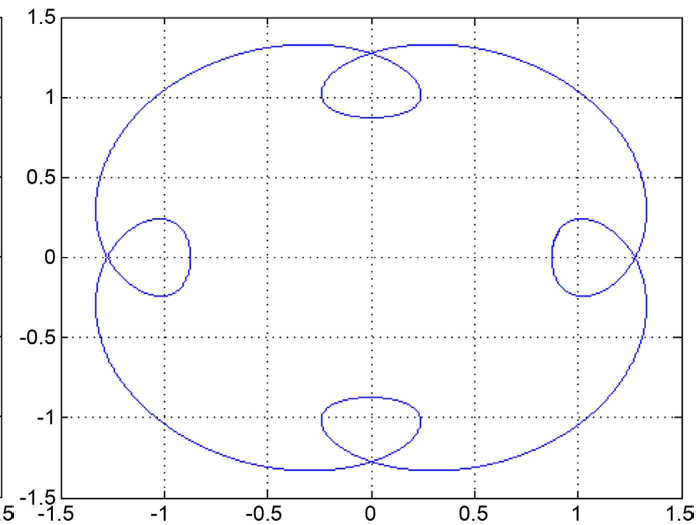

(h) $q = 0.995$, four loops periodic orbit.

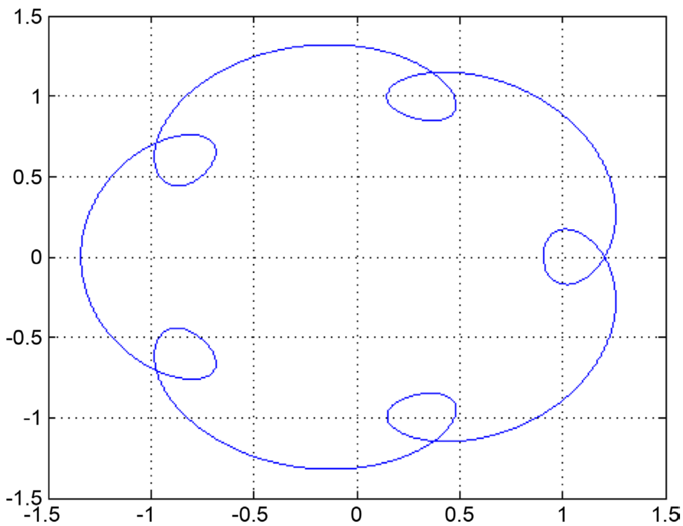

(i) $q = 0.9845$, five loops periodic orbit.

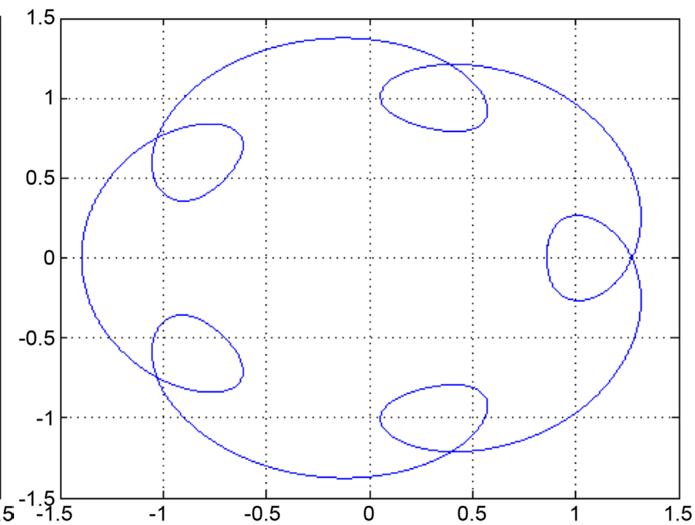

(j) $q = 0.995$, five loops periodic orbit.

Figure 4. Periodic orbits around both primaries for Sun-Earth system for $C = 2.94$.

$$a = \left[\frac{2}{r_1} - \frac{V^2}{1-\mu}\right]^{-1}, \tag{10}$$

$$e = \sqrt{1 - \frac{h^2}{a(1-\mu)}}, \tag{11}$$

where,

$$V^2 = \left(\dot{x}^2 + (\dot{y} + x + \mu)^2\right), \tag{12}$$

$$h = (x + \mu_2)(y + \dot{x} + \mu), \tag{13}$$

$$r_1^2 = (x + \mu)^2 + y^2. \tag{14}$$

Using the set of Equations (10)-(14), for different number of loops and selected values of Jacobi constant C and solar radiation pressure q, the location of the orbit, the semi major axis a and eccentricity e of the periodic orbits are calculated and numerical values are given for Sun-Mars system in Table 5.

From Table 5, it can be noticed that for a fixed number of loops, a decrease in the value of Jacobi constants from 2.96 to 2.93 cause the orbits to recede from the Mars; the semi-major axis decreases and the eccentricity of the orbit increases. Similar effects can be observed for Sun-Earth system and the numerical estimates of these effects are displayed in Table 6.

We have studied the variation of position of periodic orbits around Sun-Mars and Sun-Earth system due to the variation in solar radiation pressure and Jacobi constants C. In Figure 5 we have shown the variation of position of closed periodic orbit with one loop for solar radiation pressure in the range (0.9845, 1) for Sun-Mars system corresponding to Jacobi constants $C = 2.93$, 2.94. From Figure 5 it is clear that the position of the orbits recedes from Mars when the solar radiation pressure decreases from 0.9845 to 1 and C decreases. Note that Single-loop periodic orbits are not available for $C = 2.95$ and 2.96.

Similar kind of conclusion can be drawn from Figure 6 for the Sun-Earth system.

We have studied the effect of q and C on the position of the orbits having loops varying from 1 to 5 for both Sun-Mars and Sun-Earth systems. The results of these

Table 5. Location, semi major axis and eccentricity of orbits for $q = 1$, 0.995, 0.99 and 0.9845 for Sun-Mars system.

No. of loop	C	$q = 1$			$q = 0.995$			$q = 0.99$			$q = 0.9845$		
		x	a	e	x	a	e	x	a	e	x	a	e
1	2.96	0.983	1.5880	0.3809	0.9967	1.57075	0.36546	-	-	-	-	-	-
	2.95	0.96791	1.58760	0.39033	0.98115	1.56765	0.37412	0.9949	1.55014	0.35818	-	-	-
	2.94	0.95327	1.58765	0.39957	0.96607	1.56716	0.38355	0.97935	1.54801	0.36735	0.99455	1.52940	0.34971
	2.93	0.939	1.58755	0.40852	0.95139	1.56664	0.39272	0.96424	1.54709	0.37674	0.97891	1.52685	0.35887
2	2.96	0.94152	1.31045	0.28153	0.95985	1.29725	0.26009	0.97957	1.28508	0.23774	-	-	-
	2.95	0.92255	1.31045	0.296010	0.93971	1.29672	0.27532	0.95807	1.28401	0.25384	0.97992	1.27131	0.22921
	2.94	0.90454	1.31044	0.30974	0.92071	1.29630	0.28974	0.93792	1.28318	0.26907	0.95825	1.26990	0.24541
	2.93	0.88737	1.31042	0.32284	0.90269	1.29594	0.30345	0.91891	1.28245	0.28347	0.93795	1.26869	0.26069
3	2.96	0.91532	1.21146	0.24445	0.9363	1.19999	0.21974	0.95957	1.18956	0.19334	0.98875	1.17987	0.16199
	2.95	0.89429	1.21146	0.26180	0.91353	1.19959	0.23846	0.93455	1.18863	0.21376	0.96036	1.17776	0.18459
	2.94	0.87465	1.21143	0.278004	0.89248	1.19919	0.25576	0.91175	1.18783	0.23242	0.93506	1.17645	0.20519
	2.93	0.85619	1.21144	0.29324	0.87283	1.19880	0.27191	0.89069	1.18710	0.24969	0.91204	1.17526	0.22397
4	2.96	0.89707	1.16044	0.22696	0.91959	1.14979	0.20021	0.9451	1.14015	0.17108	0.9783	1.13112	0.13511
	2.95	0.87494	1.16043	0.24602	0.89529	1.14929	0.22107	0.91785	1.13925	0.19434	0.9462	1.12931	0.16214
	2.94	0.8545	1.16042	0.26363	0.87314	1.14898	0.24008	0.89353	1.13847	0.21515	0.91857	1.12798	0.18565
	2.93	0.835433	1.16042	0.28006	0.852695	1.14862	0.25763	0.871375	1.13772	0.23411	0.89397	1.12678	0.20662
5	2.96	0.883675	1.12928	0.21749	0.90711	1.11910	0.18943	0.93405	1.10990	0.15844	0.9701	1.10120	0.11906
	2.95	0.86093	1.12926	0.237620	0.8819	1.11869	0.21167	0.90538	1.10902	0.18362	0.93535	1.09956	0.14934
	2.94	0.84007	1.12925	0.25608	0.85915	1.11830	0.23173	0.88016	1.10824	0.20581	0.90623	1.09825	0.17485
	2.93	0.820715	1.12926	0.27323	0.83829	1.11794	0.25015	0.8574	1.10749	0.22582	0.88069	1.09705	0.19722

Table 6. Location, semi major axis and eccentricity of orbits for $q = 1$, 0.995, 0.99 and 0.9845 for Sun-Earth system.

No. of loop	C	$q = 1$			$q = 0.995$			$q = 0.99$			$q = 0.9845$		
		x	a	e	x	a	e	x	a	e	x	a	e
	2.96	0.98305	1.59310	0.38293	-	-	-	-	-	-	-	-	-
1	2.95	0.96795	1.59008	0.39126	0.9812	1.57215	0.37589	0.9949603	1.56800	0.36546	-	-	-
	2.94	0.9533	1.58919	0.40013	0.9661	1.56937	0.38440	0.9794	1.55205	0.36896	0.994601	1.54580	0.35658
	2.93	0.93904	1.58875	0.40895	0.95142	1.56808	0.39326	0.96425	1.54897	0.37749	0.97895	1.53065	0.36044
	2.96	0.94157	1.31144	0.28204	0.9599	1.29882	0.26095	-			-		
2	2.95	0.92259	1.31111	0.29634	0.93975	1.29762	0.27579	0.95813	1.28554	0.25469	0.98	1.27517	0.23148
	2.94	0.90456	1.31087	0.30996	0.92075	1.29693	0.29006	0.93796	1.28404	0.26953	0.9583	1.27138	0.24626
	2.93	0.8874	1.31080	0.32301	0.90273	1.29643	0.30368	0.91895	1.28305	0.28378	0.938	1.26958	0.26118
	2.96	0.91538	1.21204	0.24477	0.93635	1.20078	0.22022	0.95965	1.19115	0.19436	-		
3	2.95	0.89434	1.21187	0.26202	0.91359	1.20015	0.23878	0.93462	1.18946	0.21426	0.96045	1.17944	0.18568
	2.94	0.87469	1.21174	0.27816	0.89252	1.19956	0.25597	0.91181	1.18837	0.23273	0.93513	1.17729	0.20570
	2.93	0.85623	1.21170	0.29337	0.87287	1.19910	0.27207	0.89074	1.18748	0.24990	0.9121	1.17580	0.22428
	2.96	0.89714	1.16088	0.22720	0.91965	1.15036	0.20057	0.9452	1.14124	0.17179	0.97844	1.13506	0.13800
4	2.95	0.87499	1.16073	0.24618	0.89535	1.14980	0.22130	0.91793	1.13986	0.19471	0.9463	1.13042	0.16289
	2.94	0.85454	1.16065	0.26375	0.8732	1.14930	0.24024	0.89359	1.13886	0.21538	0.91865	1.12859	0.18603
	2.93	0.83547	1.16061	0.28015	0.85274	1.14886	0.25776	0.87142	1.13800	0.23426	0.89403	1.12717	0.20685
	2.96	0.88373	1.12961	0.21768	0.90719	1.11959	0.18973	0.93415	1.11072	0.15899	0.9703	1.10404	0.12116
5	2.95	0.86099	1.12953	0.23776	0.88195	1.11899	0.21185	0.90546	1.10950	0.18392	0.93547	1.1004	0.14994
	2.94	0.84012	1.12947	0.25619	0.8592	1.11854	0.23187	0.88022	1.10856	0.20599	0.9063	1.09871	0.17514
	2.93	0.82075	1.12942	0.27331	0.83833	1.11813	0.25024	0.85745	1.10773	0.22595	0.88075	1.09736	0.19740

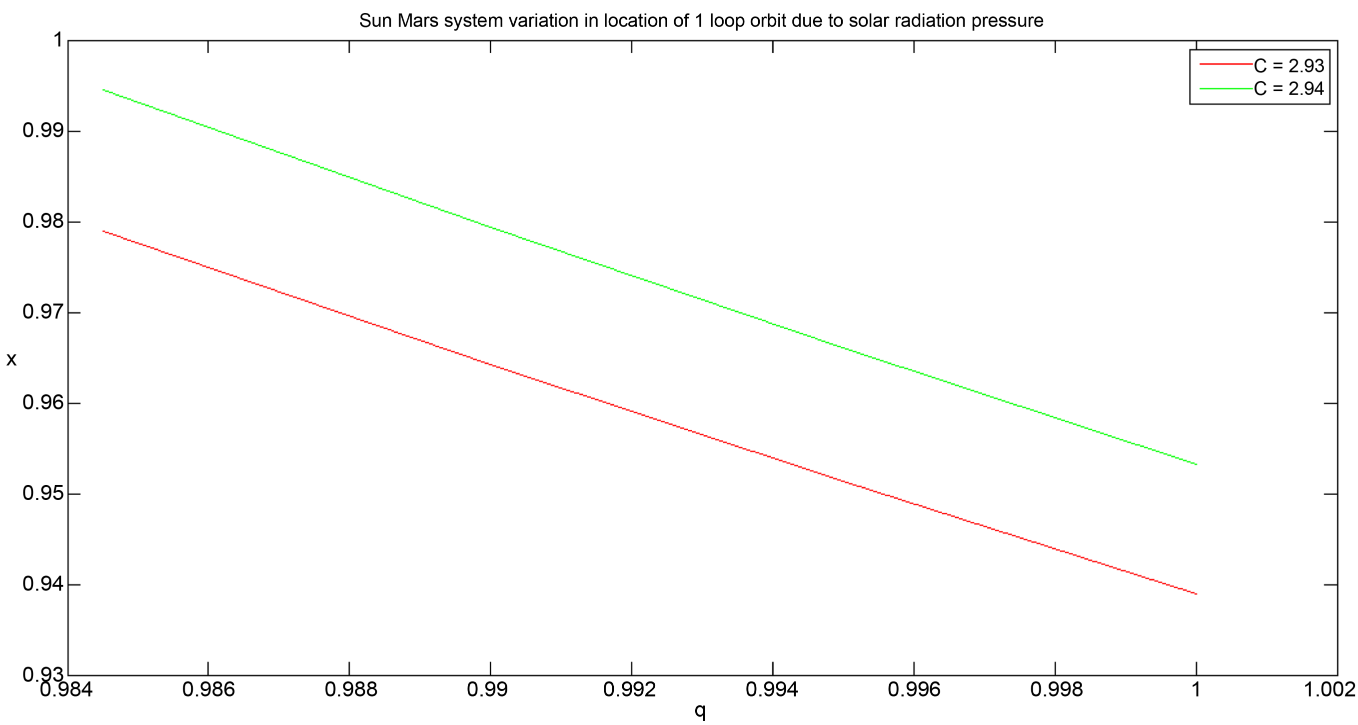

Figure 5. Variation in location of single loop periodic orbit around Sun-Mars system due to solar radiation pressure.

observations for 5 loops closed periodic orbit in both Sun-Mars and Sun-Earth systems are shown in Figure 7 and Figure 8.

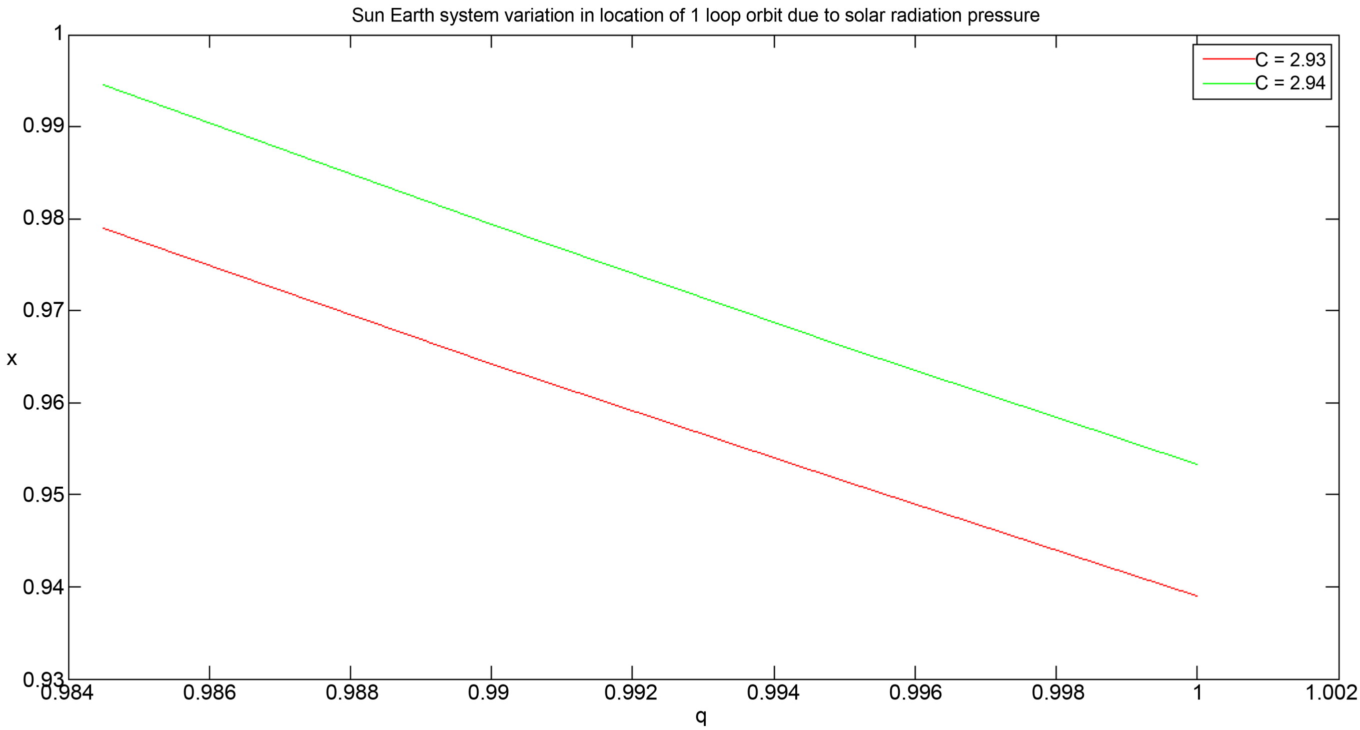

Figure 6. Variation in location of one loop periodic orbit around Sun-Earth due to solar radiation pressure.

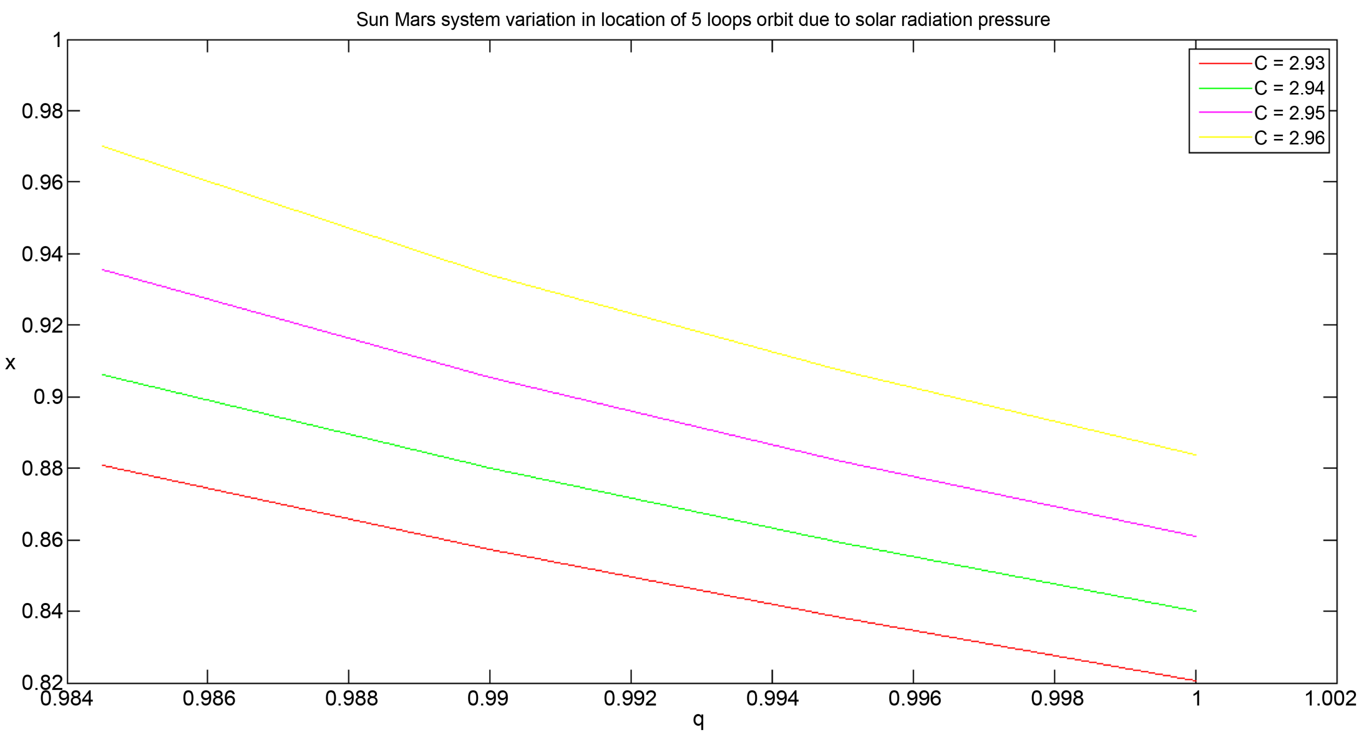

Figure 7. Variation in location of five loops periodic orbit around Sun-Mars system due to solar radiation pressure.

From Figure 9 and Figure 10, it can be observed that for given solar radiation pressure, location of periodic orbit moves away from second primary as number of loops in

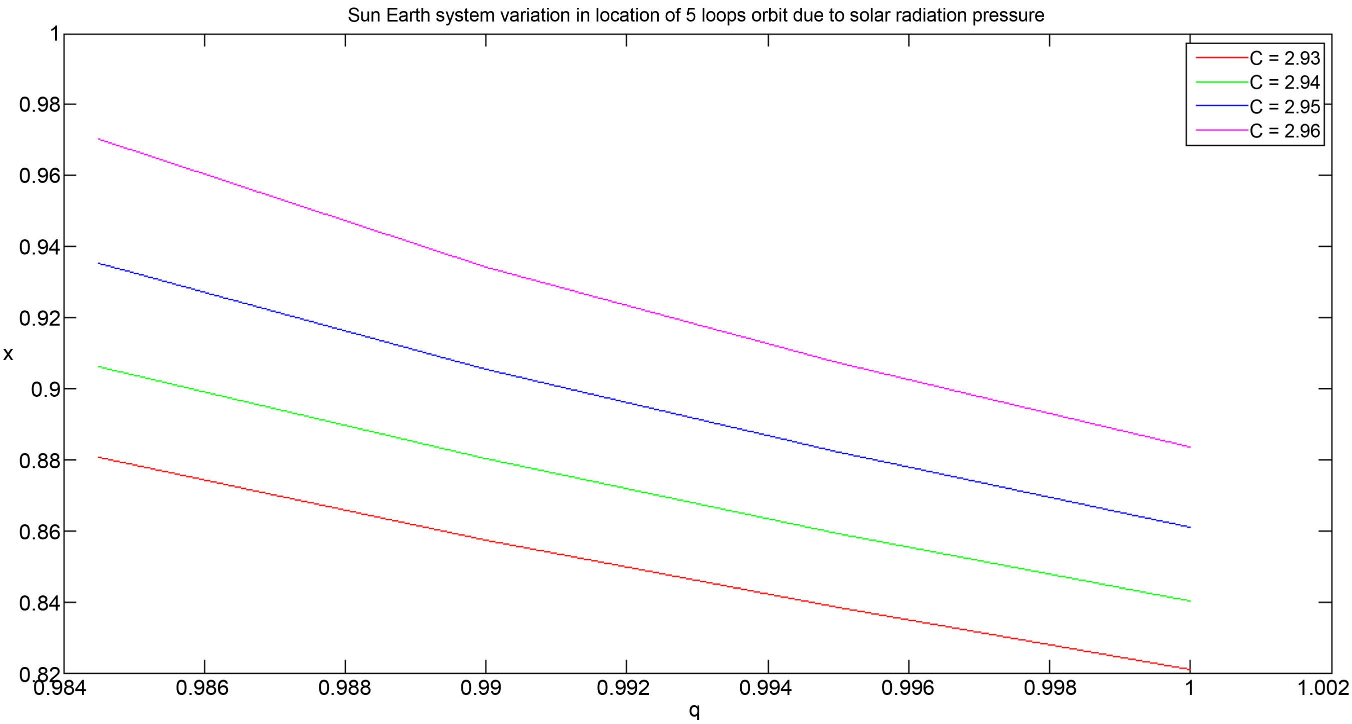

Figure 8. Variation in location of five loops periodic orbit around Sun-Earth system due to solar radiation pressure.

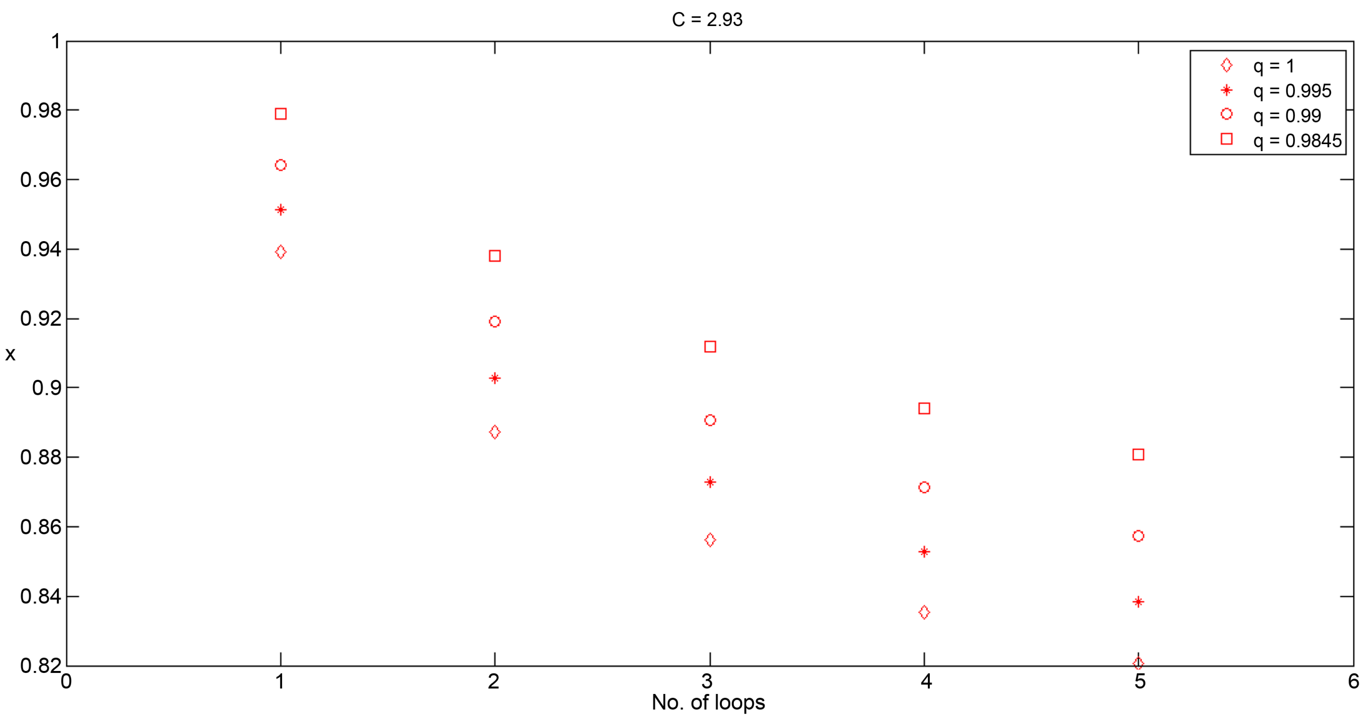

Figure 9. Variation in location of periodic orbit around Sun-Mars system for $C = 2.93$ due to number of loops for different solar radiation pressure.

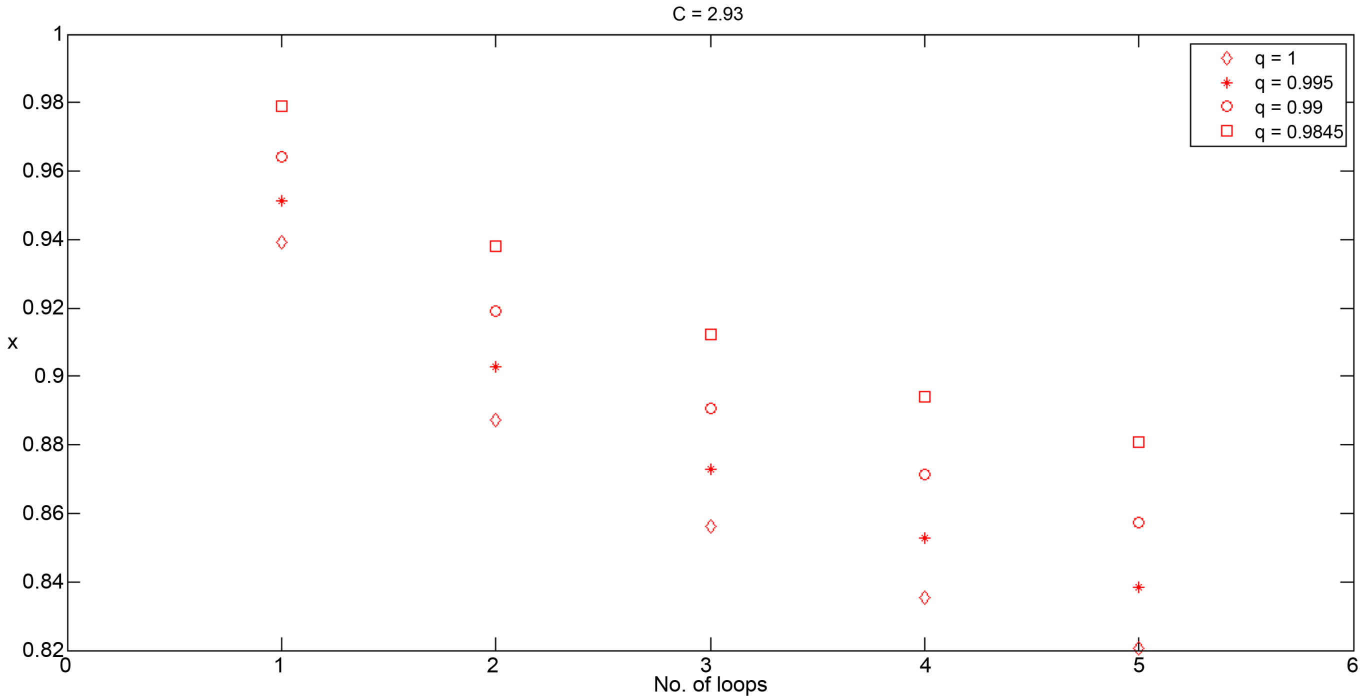

Figure 10. Variation in location of periodic orbit around Sun-Earth system for $C = 2.93$ due to number of loops for different solar radiation pressure.

periodic orbit increase. Also, as solar radiation pressure increases from 1 to 0.9845, location of periodic orbit moves towards second primary.

We have examined the effect of solar radiation pressure q for different values of Jacobi constants C on the semi major axis of periodic orbits with single loop and 5-loops of Sun-Mars and Sun-Earth systems. The results of these effects are displayed in Figures 11-14. While there are significant changes in the semi major axis due to solar radiation pressure, the effect of C on the semi-major axis is less in comparison with that of q. Figures 11-14 indicate that the semi major axis decreases as solar radiation pressure increases from 1 to 0.9845. Figure 12 shows behavior of semi major axis of single loop periodic orbit for different solar radiation pressure. Green curve indicates variation of semi major axis for $C = 2.94$. It shows non smooth behavior near $q = 0.99$, because single loop periodic orbit for $C = 2.94$ and $q = 0.9845$ is located at $x = 0.994601$ loses its periodicity after time $t = 110$. Figure 14 shows behavior of semi major axis of five loops periodic orbits for different q. Magenta curve indicates variation for semi major axis for $C = 2.96$. It shows non smooth behavior near $q = 0.99$, because five loops periodic orbit for $C = 2.96$ and $q = 0.9845$ is located at $x = 0.9703$ loses its periodicity after time $t = 500$.

The variation of semi major axis against the number of loops is examined for different solar radiation pressure and the results of the study are displayed in Figure 15 and Figure 16. The semi major axis decreases with increase in the number of loops. Further for a fixed number of loops, the semi-major axes decreases with increase in solar radiation pressure from 1 to 0.9845.

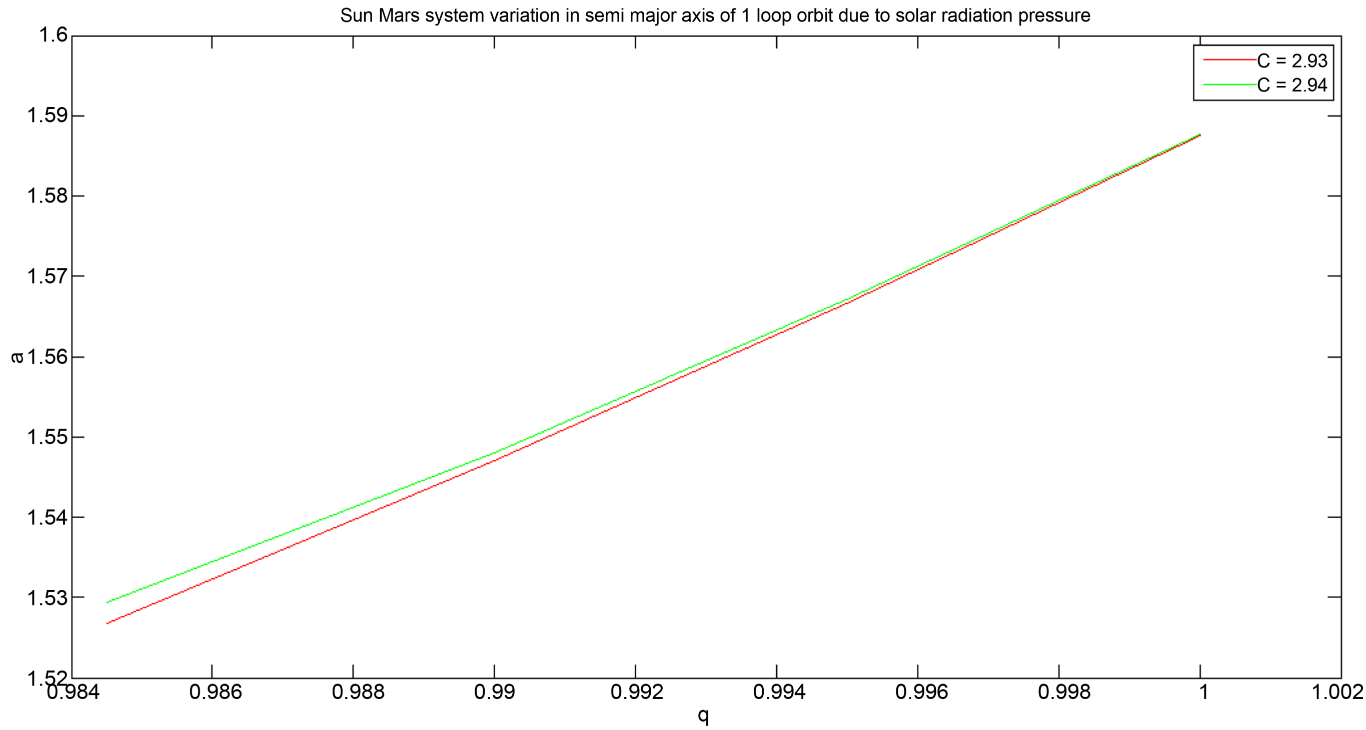

Figure 11. Variation in semi major axis of one loop periodic orbit around Sun-Mars system due to solar radiation pressure.

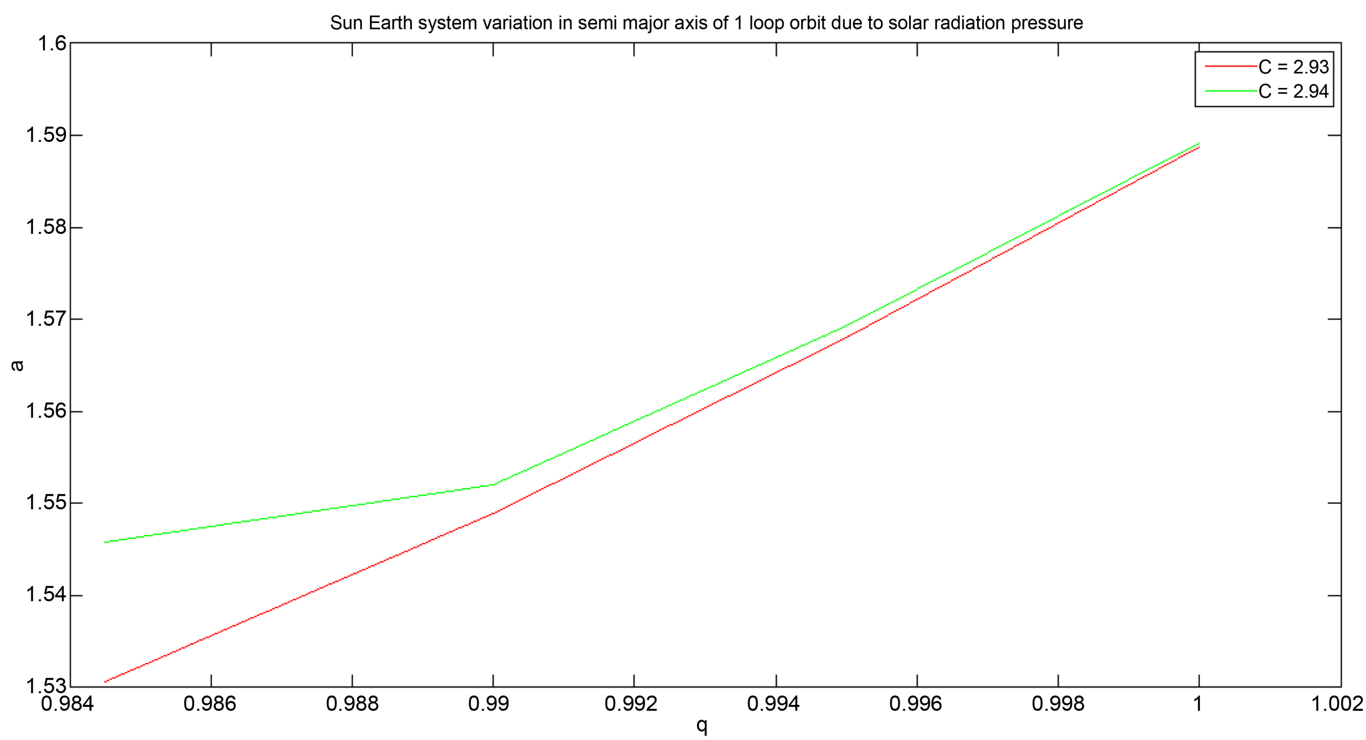

Figure 12. Variation in semi major axis of one loop periodic orbit around Sun-Earth system due to solar radiation pressure.

From Figure 15 and Figure 16 it can be observed that, for given pair of C and q, as the number of loops increases in periodic orbit, semi major axis decreases. Also, as solar

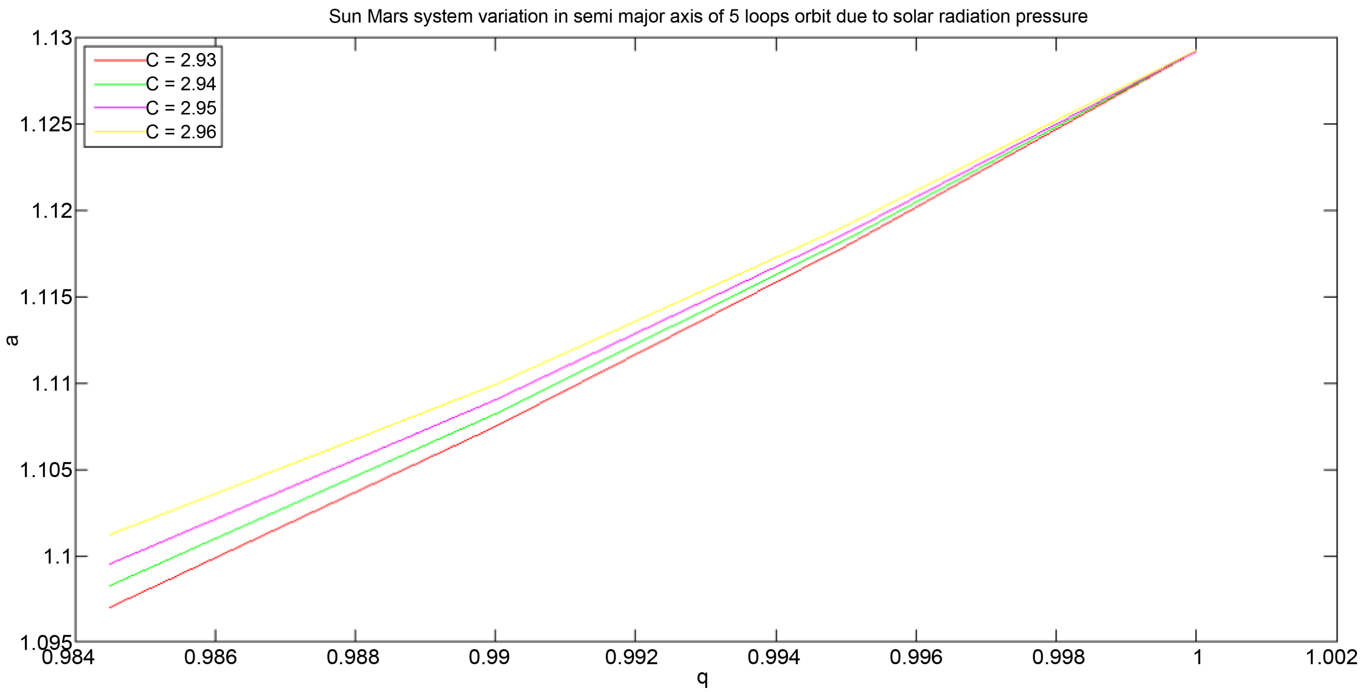

Figure 13. Variation in semi major axis of five loops periodic orbit around Sun-Mars system due to solar radiation pressure.

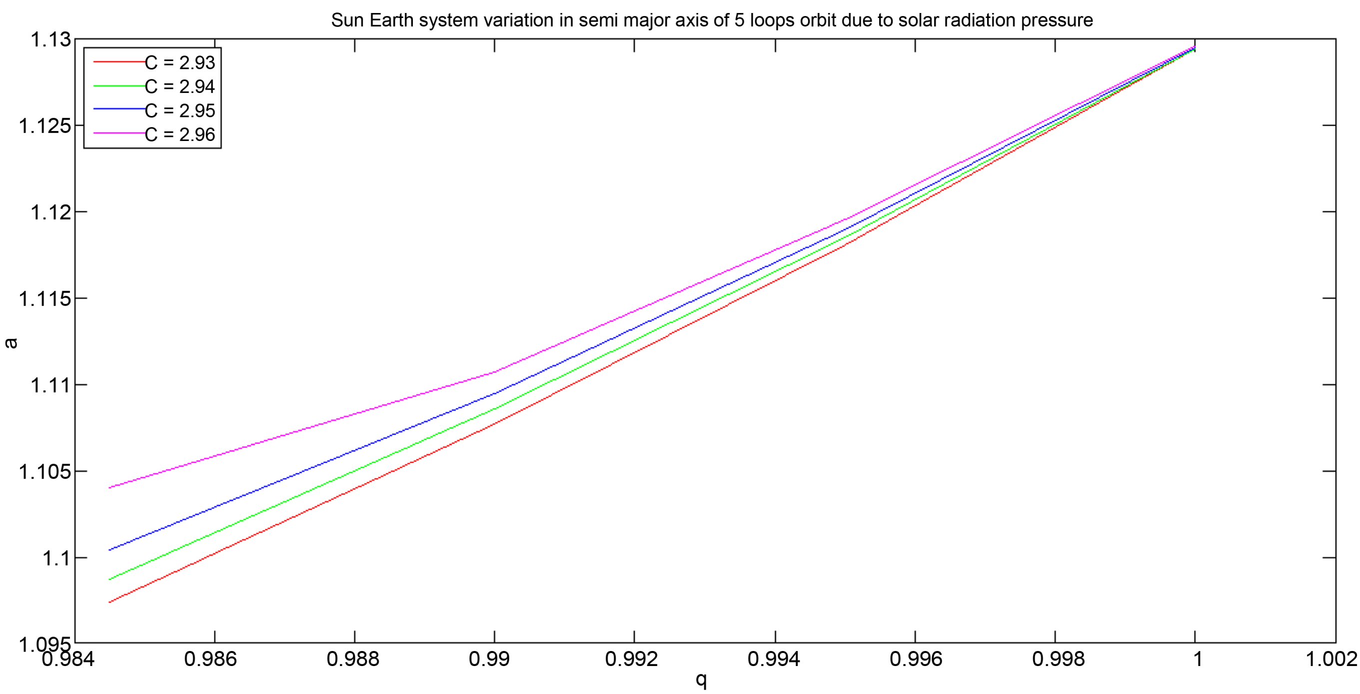

Figure 14. Variation in semi major axis of five loops periodic orbit around Sun-Earth system due to solar radiation pressure.

radiation pressure increases from 1 to 0.9845 semi major axis of periodic orbit for given loop decreases.

The variations of the other geometric parameter, viz, eccentricity e with respect to solar radiation pressure q and Jacobi constant C for single and five loops periodic orbits

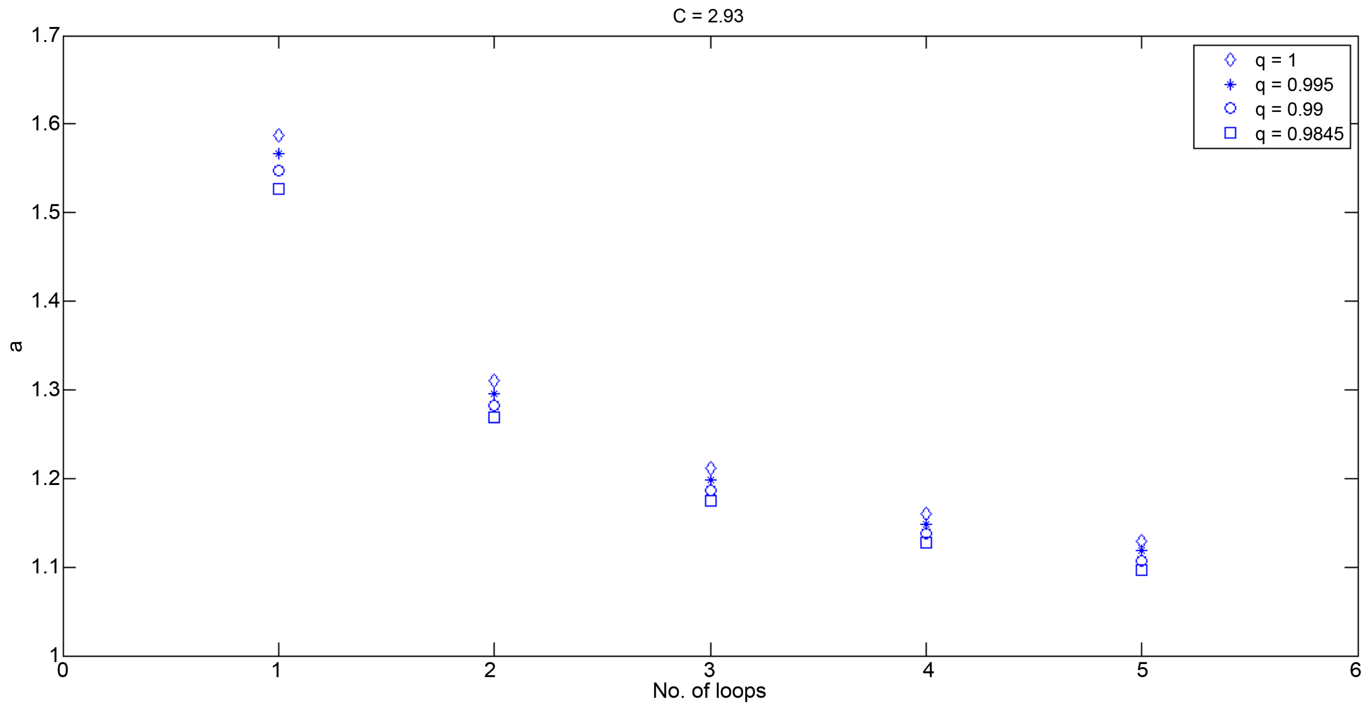

Figure 15. Variation in semi major axis of periodic orbit around Sun-Mars system due to number of loops for $C = 2.93$.

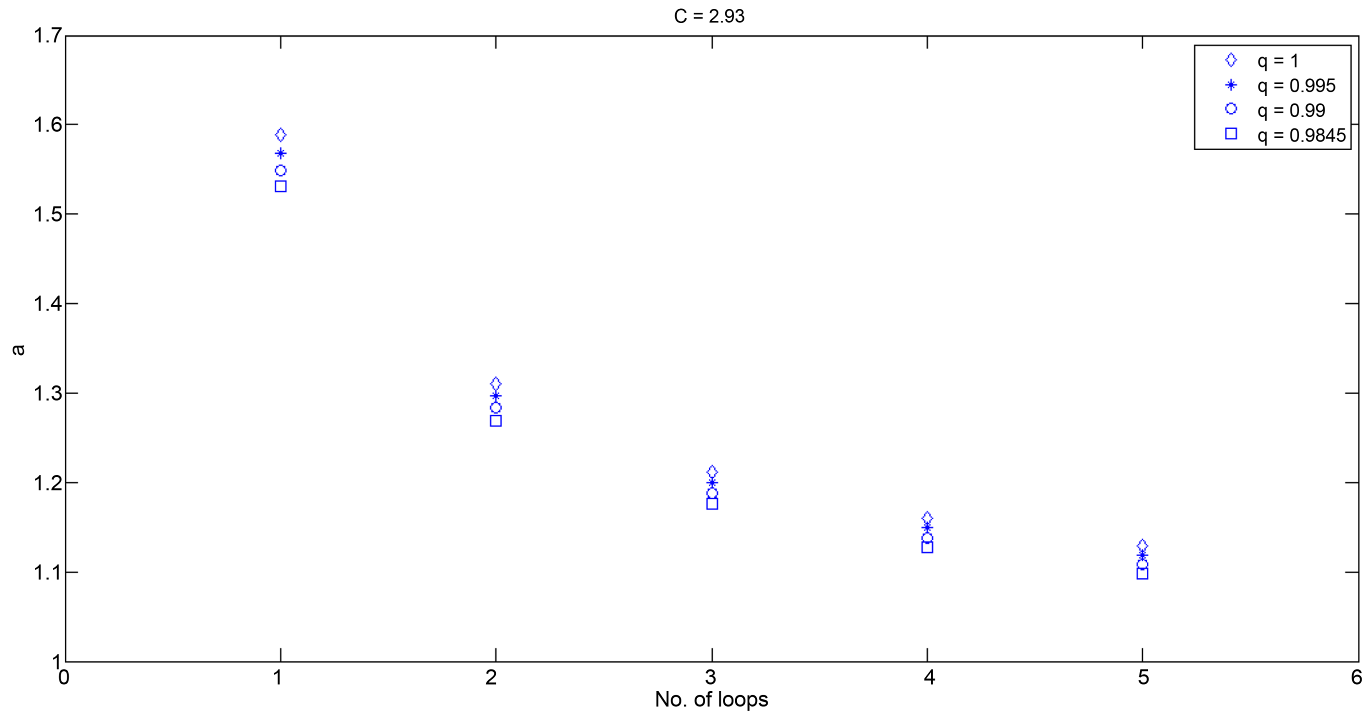

Figure 16. Variation in semi major axis of periodic orbit around Sun-Earth system due to number of loops.

are shown in Figures 17-20 for both Sun-Mars and Sun-Earth systems. The eccentricity decreases as q increases from 1 to 0.9845 and decreases as C increases for single loop periodic orbit for both systems Sun-Mars and Sun-Earth as shown in Figure 17 and

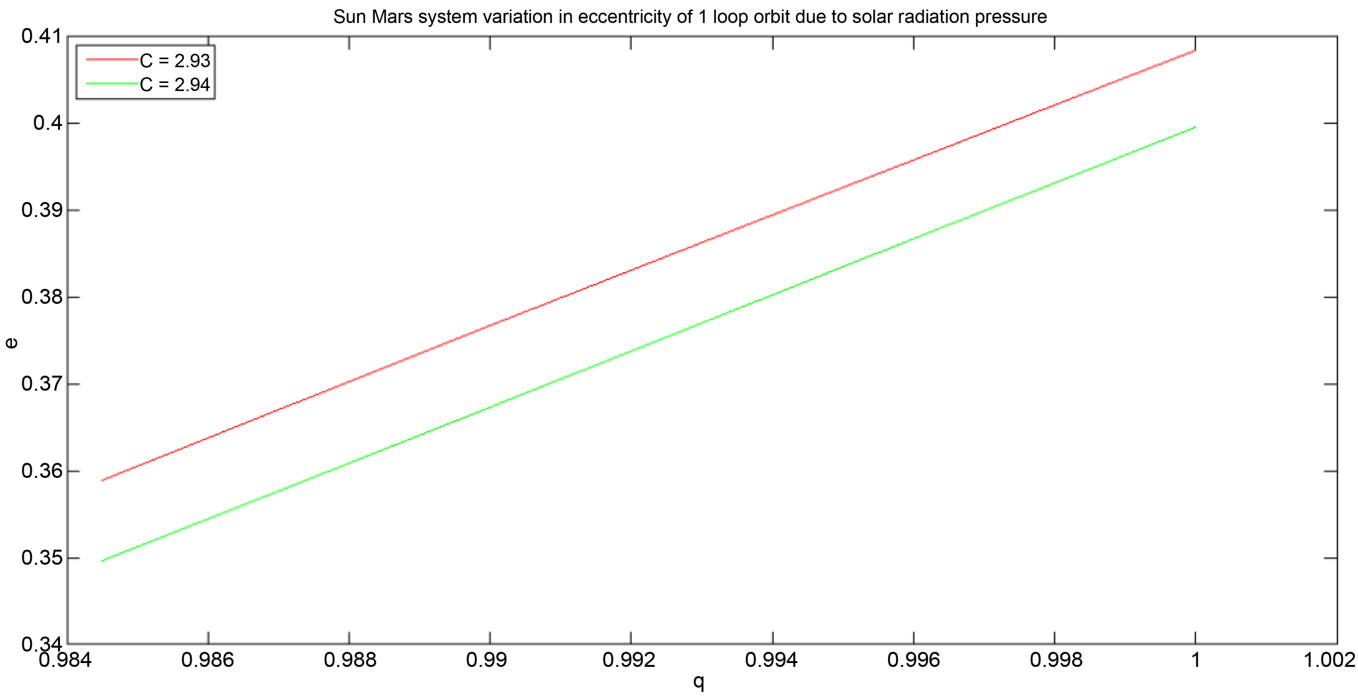

Figure 17. Variation in eccentricity of single loop periodic orbit around Sun-Mars system due to solar radiation pressure.

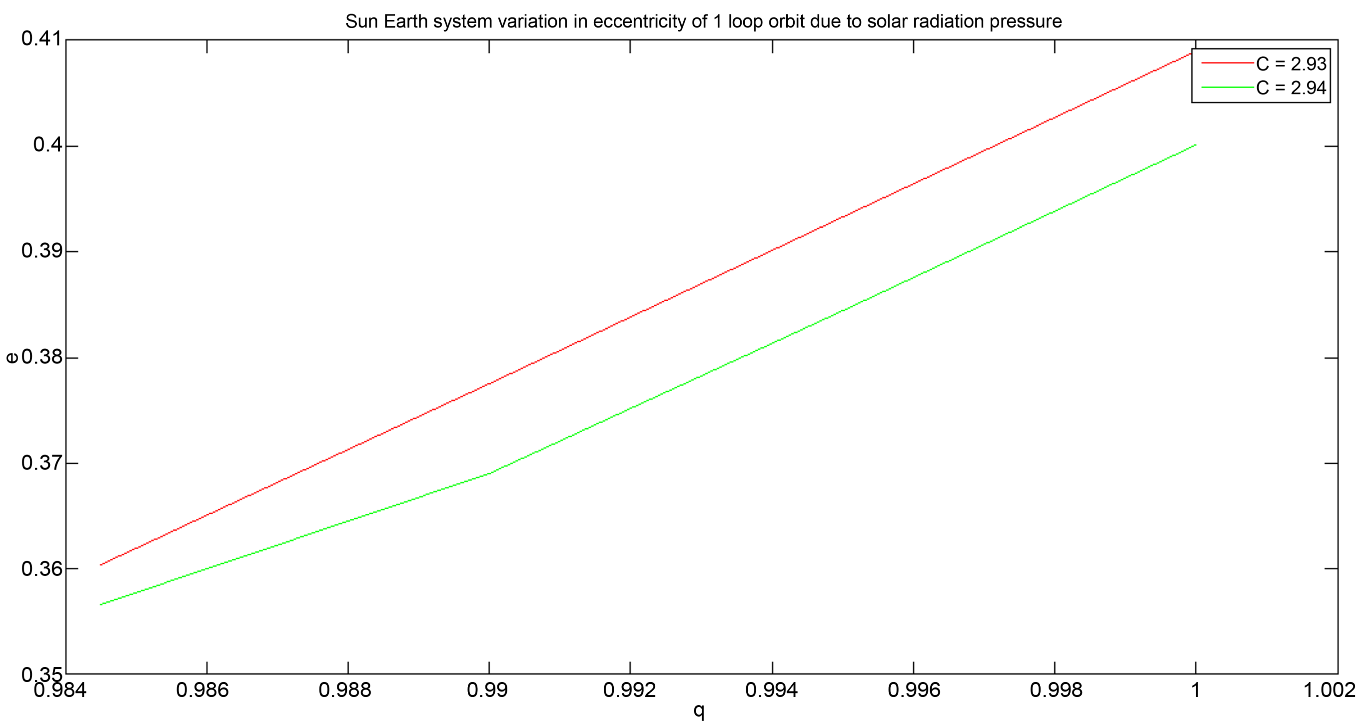

Figure 18. Variation in eccentricity of single loop periodic orbit around Sun and Earth due to oblateness.

Figure 18. Here we can observe that effect of orbits which lost their periodicity after some time is less on eccentricity of the periodic orbit in comparison of semi major axis of the periodic orbit. Figure 18 shows variation in eccentricity of single loop orbit

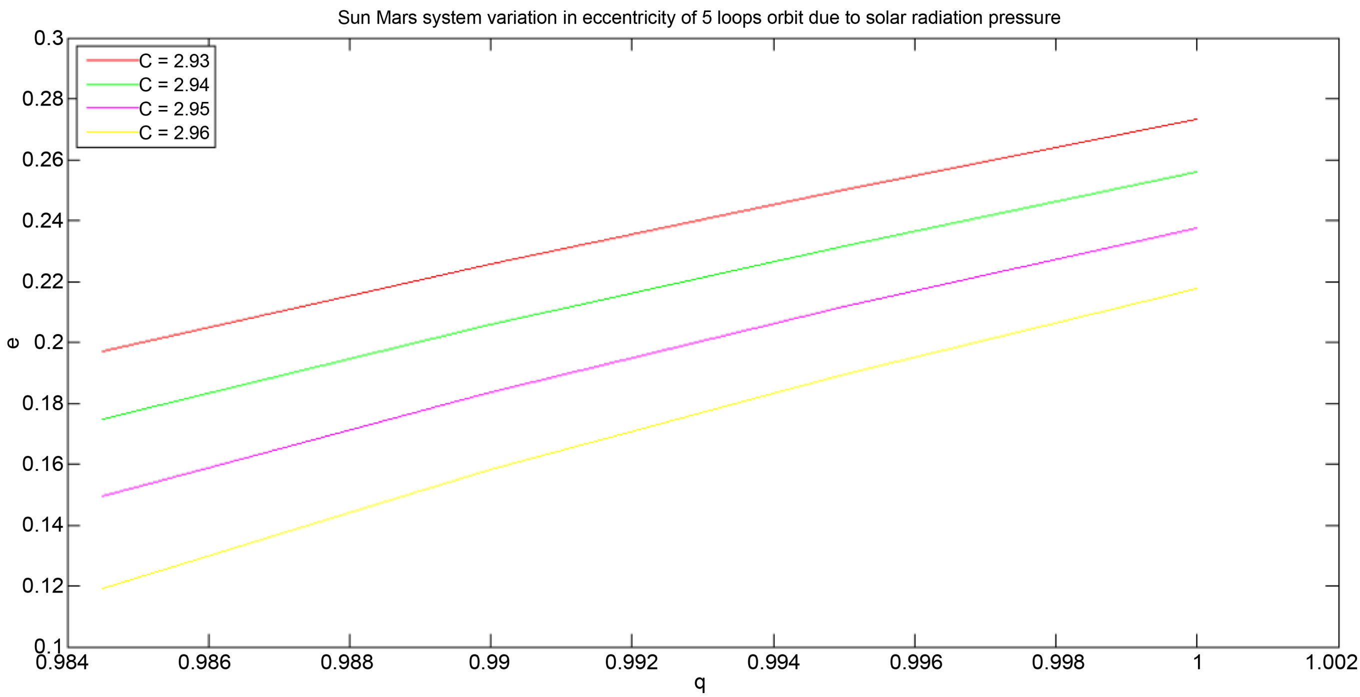

Figure 19. Variation in eccentricity of five loops periodic orbit around Sun-Mars system due to solar radiation pressure.

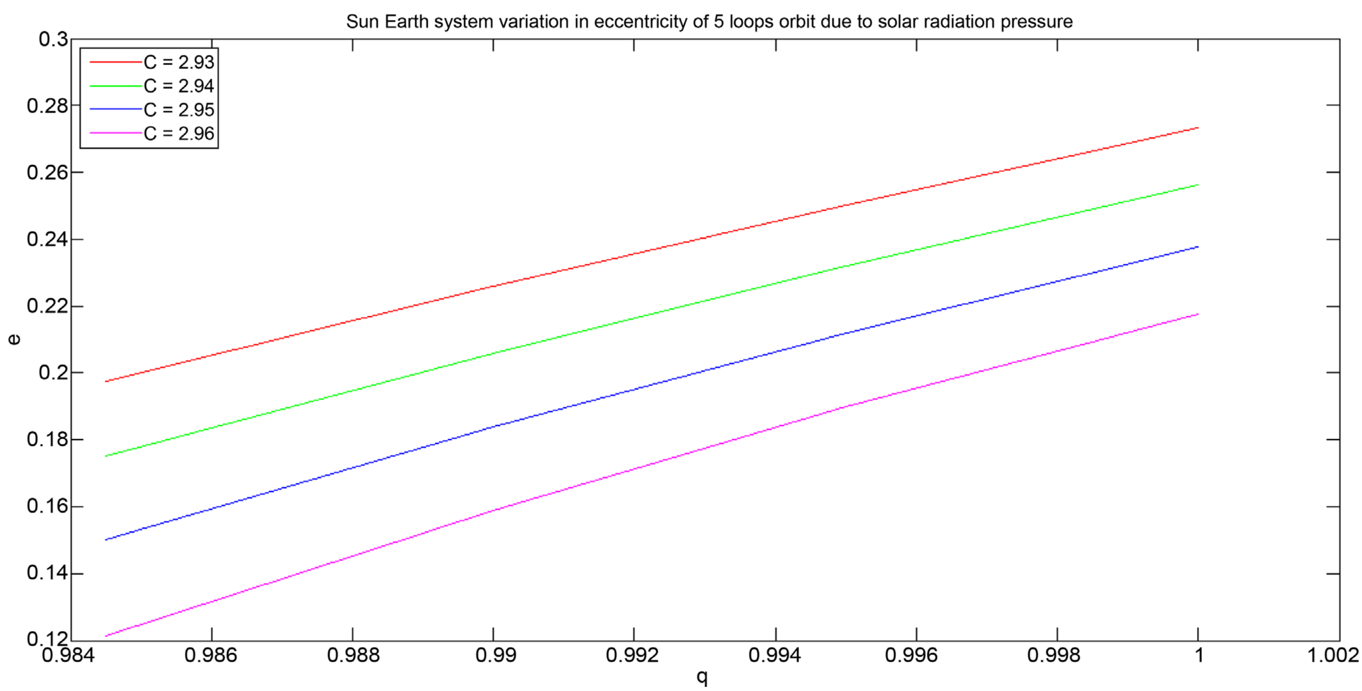

Figure 20. Variation in eccentricity of five loops periodic orbit around Sun-Earth system due to solar radiation pressure.

corresponding to variation in q for given C. green curve shows non smooth behavior corresponding to periodic orbit for $C = 2.94$, $q = 0.9845$ which is located at $x = 0.994601$, loses its periodicity after $t = 110$.

We have also analyzed the effect of number of loops on the eccentricity of the orbit.

These effects are depicted in Figure 21 and Figure 22. It is found that the eccentricity decreases as number of loops increases. For a given loop, the eccentricity is found to decrease as solar radiation pressure increases 1 to 0.9845.

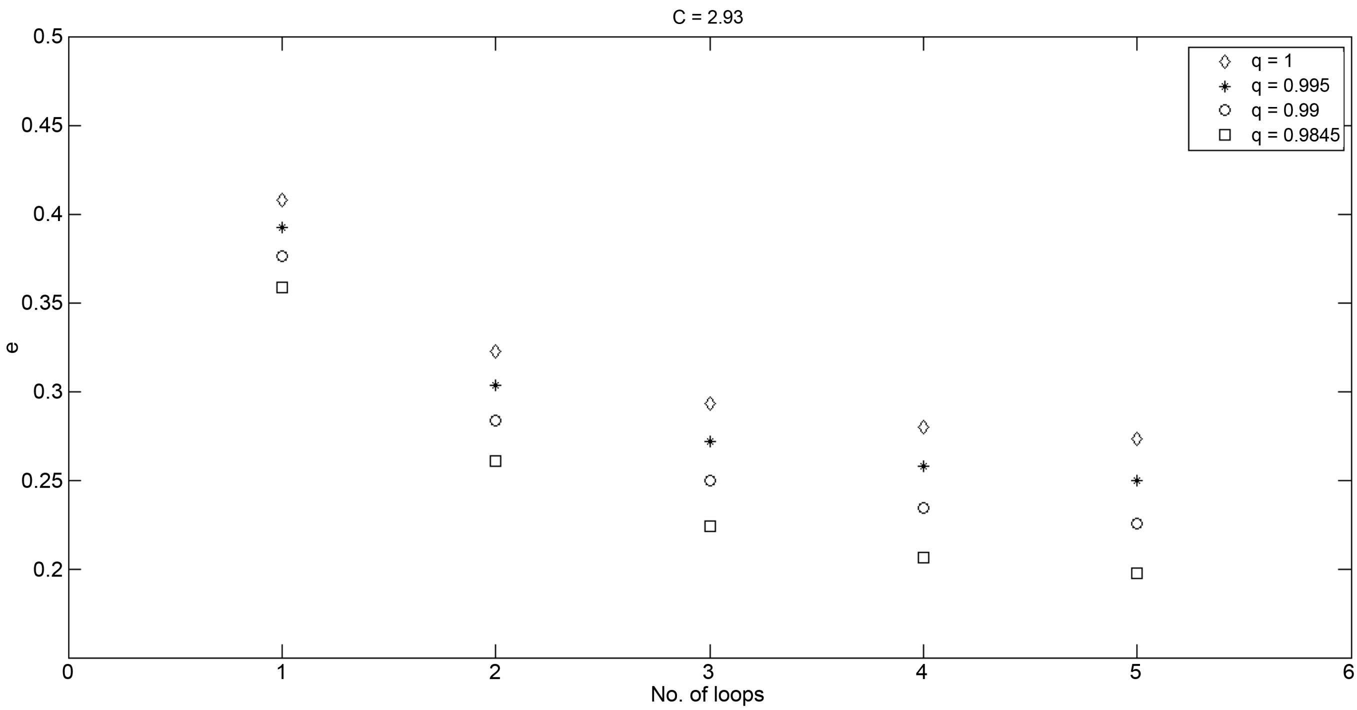

Figure 21. Variation in eccentricity of periodic orbit around Sun-Mars system due to number of loops.

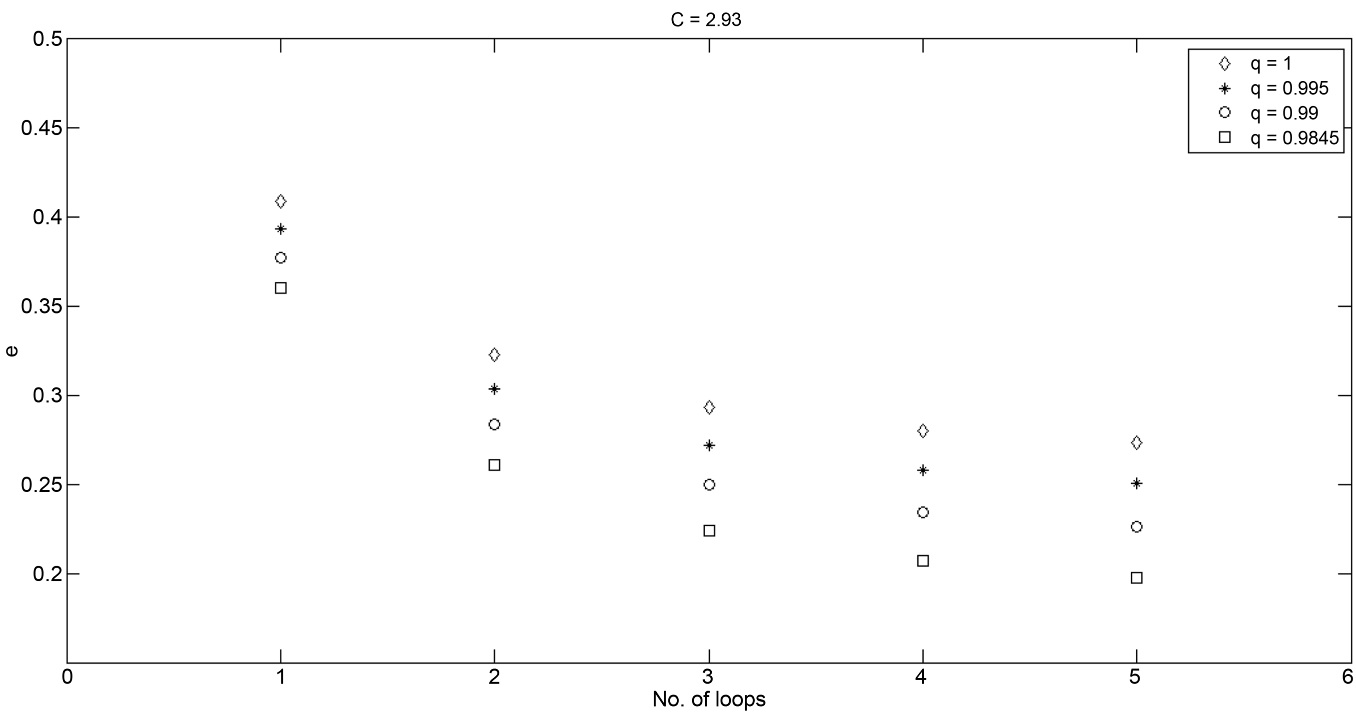

Figure 22. Variation in eccentricity of periodic orbit around Sun and Earth due to number of loops.

In Table 5 initial velocity of secondary body is denoted by V, D_1 and D_2 are the distance of secondary body from Mars and Sun respectively. V is in kms^{-1}, D_1 and D_2 are in km. Similar notations are used in Table 6 also. In Table 6 distance of secondary body from Earth is denoted by D_1. V can be obtained using Equation (11).

The conversion from units of distance (I) and velocity (J) in the normalized dimension less system to the dimensionalized system is given by,

$$\text{Distance } D = L \times I, \tag{14}$$

$$\text{Velocity } V = O \times J. \tag{15}$$

where L is the distance between the centers of both primaries in km. O is the orbital velocity of second primary around first primary [12]. For Sun Mars and Sun Earth system L = 227,940,000 and 149,600,000 km respectively. Mean orbital velocity of Mars around Sun and Earth around Sun are 24.07 km·sec^{-1} and 29.78 km·sec^{-1} respectively.

It can be observed from Table 7 and Table 8 that for given solar radiation pressure and given loop orbit as C decreases, V and D_1 increases and D_2 decreases. For given C and given number of loop as q increases from 1 to 0.9845 initial velocity V and D_1 decreases and D_2 increases. So, the effect of Jacobi constant C and solar radiation pressure

Table 7. Location, velocity and distance of orbit from both primaries for q = 1, 0.995, 0.99, 0.9845 for Sun-Mars system.

No. of loop	C	q = 1				q = 0.995				q = 0.99				q = 0.9845			
		x	V (km·sec^{-1})	D_1 (10^7 km)	D_2 (10^8 km)	x	V (km·sec^{-1})	D_1 (10^7 km)	D_2 (10^8 km)	x	V (km·sec^{-1})	D_1 (10^7 km)	D_2 (10^8 km)	x	V (km·sec^{-1})	D_1 (10^7 km)	D_2 (10^8 km)
1	2.96	0.983	28.52	0.38749	2.24065	0.9967	28.17	**0.07521**	2.27187	-	-	-	-	-	-	-	-
	2.95	0.96791	28.84	0.73145	2.20625	0.98115	28.48	0.42965	2.23643	0.9949	28.12	0.11624	2.26777	-	-	-	-
	2.94	0.95327	29.16	1.06515	2.17288	0.96607	28.80	0.77339	2.20206	0.97935	28.44	0.47068	2.23233	0.99455	28.04	0.12421	2.26697
	2.93	0.939	29.47	1.39042	2.14035	0.95139	29.12	1.10800	2.16859	0.96424	28.76	0.81510	2.19788	0.97891	28.35	0.48071	2.23132
2	2.96	0.94152	28.08	1.33298	2.14610	0.95985	27.57	0.91517	2.18788	0.97957	27.05	0.46567	2.23283	-	-	-	-
	2.95	0.92255	28.52	1.76538	2.10286	0.93971	28.04	1.37424	2.14197	0.95807	27.53	0.95574	2.18382	0.97992	26.95	0.45769	2.23363
	2.94	0.90454	28.96	2.17590	2.06180	0.92071	28.48	1.80732	2.09866	0.93792	27.99	1.41504	2.13789	0.95825	28.05	0.95164	2.18423
	2.93	0.88737	29.38	2.56728	2.02267	0.90269	28.92	2.21807	2.05759	0.91891	28.44	1.84835	2.09456	0.93795	27.90	1.41436	2.13796
3	2.96	0.91532	28.06	1.93018	2.08638	0.9363	27.47	1.45197	2.13420	0.95957	26.84	0.92155	2.18724	0.98875	26.09	2.56425	2.25375
	2.95	0.89429	28.59	2.40954	2.03844	0.91353	28.02	1.97098	2.08230	0.93455	27.43	1.49185	2.13021	0.96036	26.73	0.90354	2.18904
	2.94	0.87465	29.09	2.85722	1.99367	0.89248	28.55	2.45080	2.03431	0.91175	27.98	2.01156	2.07824	0.93506	27.32	1.48023	2.13137
	2.93	0.85619	29.58	3.27799	1.95160	0.87283	29.05	2.89870	1.98952	0.89069	28.51	2.49160	2.03023	0.91204	27.88	2.00495	2.07890
4	2.96	0.89707	28.14	2.34617	2.04478	0.91959	27.49	1.83285	2.09611	0.9451	26.79	1.25138	2.15426	0.9783	25.92	4.94622	2.22993
	2.95	0.87494	28.72	2.85061	1.99433	0.89529	28.12	2.45080	2.03431	0.91785	27.45	1.87251	2.09214	0.9462	26.67	1.22630	2.15676
	2.94	0.8545	29.27	3.31651	1.94774	0.87314	28.68	2.89163	1.99023	0.89353	28.06	2.42686	2.03671	0.91857	27.34	1.85610	2.09378
	2.93	0.835433	29.79	3.75113	1.90428	0.852695	29.23	3.35766	1.94363	0.871375	28.64	2.93187	1.98621	0.89397	27.96	2.41684	2.03771
5	2.96	0.883675	28.25	2.65150	2.01424	0.90711	27.56	2.11732	2.06766	0.93405	26.80	1.50325	2.12907	0.9701	25.85	6.81533	2.21124
	2.95	0.86093	28.85	3.16995	1.96240	0.8819	28.11	2.38675	2.04072	0.90538	27.52	2.15676	2.06372	0.93535	26.68	1.47362	2.13203
	2.94	0.84007	29.43	3.64543	1.91485	0.85915	28.82	3.21052	1.95834	0.88016	28.17	2.73162	2.00623	0.90623	27.40	2.13738	2.06566
	2.93	0.820715	29.98	4.08672	1.87072	0.83829	29.39	3.68601	1.91079	0.8574	28.78	3.25041	1.95435	0.88069	28.06	2.71954	2.00744

Table 8. Location, velocity and distance of orbit from both primaries for $q = 1, 0.995, 0.99, 0.9845$ for Sun-Earth system.

No. of loop	C	$q = 1$				$q = 0.995$				$q = 0.99$				$q = 0.9845$			
		x	V (km·sec^{-1})	D_1 (10^7 km)	D_2 (10^8 km)	x	V (km·sec^{-1})	D_1 (10^7 km)	D_2 (10^8 km)	x	V (km·sec^{-1})	D_1 (10^7 km)	D_2 (10^8 km)	x	V (km·sec^{-1})	D_1 (10^7 km)	D_2 (10^8 km)
1	2.96	0.98305	35.32	0.25352	1.47064	-	-	-	-	-	-	-	-	-	-	-	-
	2.95	0.96795	35.70	0.47942	1.44805	0.9812	35.26	0.28120	1.46787	0.9949603	34.88	**0.07535**	1.48846	-	-	-	-
	2.94	0.9533	36.09	0.69858	1.42614	0.9661	35.64	0.50709	1.44529	0.9794	35.20	0.30813	1.46518	0.994601	34.77	0.08072	1.48792
	2.93	0.93904	36.47	0.91191	1.40480	0.95142	36.03	0.72671	1.42332	0.96425	35.59	0.53477	1.44252	0.97895	35.10	0.31486	1.46451
2	2.96	0.94157	34.74	0.87406	1.40859	0.9599	34.13	0.59985	1.43601	-	-	-	-	-			
	2.95	0.92259	35.30	1.15800	1.38019	0.93975	34.69	0.90129	1.40587	0.95813	34.07	0.62633	1.43336	0.98	33.38	2.99155	1.46608
	2.94	0.90456	35.83	1.42773	1.35322	0.92075	35.24	1.18553	1.37744	0.93796	34.64	0.97803	1.39819	0.9583	33.96	0.62378	1.43362
	2.93	0.8874	36.36	1.68445	1.32755	0.90273	35.78	1.45511	1.35048	0.91895	35.19	1.21246	1.37475	0.938	34.53	0.92747	1.40325
3	2.96	0.91538	34.72	1.26587	1.36941	0.93635	33.99	0.95215	1.40078	0.95965	33.22	6.03591	1.43564	-	-	-	-
	2.95	0.89434	35.37	1.58062	1.33793	0.91359	34.67	1.29264	1.36673	0.93462	33.94	0.97803	1.39819	0.96045	33.08	5.91623	1.43683
	2.94	0.87469	35.99	1.87459	1.30854	0.89252	35.32	1.60785	1.33521	0.91181	34.62	1.31927	1.36407	0.93513	33.81	0.97041	1.39895
	2.93	0.85623	36.60	2.15075	1.28092	0.87287	35.95	1.90181	1.30581	0.89074	35.27	1.63448	1.33255	0.9121	34.50	1.31493	1.36450
4	2.96	0.89714	34.82	1.53874	1.34212	0.91965	34.02	1.20199	1.37580	0.9452	33.15	8.19763	1.41402	0.97844	32.11	3.22492	1.46375
	2.95	0.87499	35.53	1.87010	1.30898	0.89535	34.78	1.56551	1.33944	0.91793	33.97	1.22772	1.37322	0.9463	33.01	8.03307	1.41566
	2.94	0.85454	36.21	2.17603	1.27839	0.8732	35.49	1.89688	1.30631	0.89359	34.73	1.59184	1.33681	0.91865	33.83	1.21695	1.37430
	2.93	0.83547	36.86	2.46132	1.24986	0.85274	36.16	2.20296	1.27570	0.87142	35.44	1.92351	1.30364	0.89403	34.59	1.58526	1.33747
5	2.96	0.88373	34.95	1.73935	1.32206	0.90719	34.10	1.38839	1.35716	0.93415	33.17	9.85071	1.39749	0.9703	32.01	4.44267	1.45157
	2.95	0.86099	35.70	2.08089	1.28791	0.88195	34.71	1.41427	1.35457	0.90546	34.05	1.41427	1.35457	0.93547	33.01	9.65323	1.39946
	2.94	0.84012	36.41	2.39175	1.25682	0.8592	35.65	2.10632	1.28536	0.88022	34.85	1.79186	1.31681	0.9063	33.91	1.40170	1.35582
	2.93	0.82075	37.09	2.68153	1.22784	0.83833	36.36	2.41853	1.25414	0.85745	35.60	2.13250	1.28274	0.88075	34.72	1.78393	1.31760

q is opposite in nature. For given value of q and C as number of loops increases, D_1 increases and D_2 decreases.

From Table 7, it is observed that single loop orbit for $q = 1$ is closest to Mars and this distance is 7.521×10^7 km. which is obtained using $C = 2.96$ for $q = 0.995$. Similar notations are used in Table 6 also.

Here D_1 is the distance of secondary body from Earth. From Table 8, it is observed that single loop orbit for $q = 0.99$ is closest to Earth and this distance is 7.535×10^5 km. This orbit is obtained by taking $C = 2.95$.

We have analyzed stability of periodic orbits from loop 1 to 5 for $q = 1, 0.995, 0.99$ and 0.9845. Since stability behavior is similar for all these orbits, in this paper stability analysis for two loop orbit corresponding to $q = 0.9845$ is given. Figure 23 shows stability region for $q = 0.9845$ for two loop orbits. The left and right tips of the island are plotted by red and green curves, respectively. From Figure 23 it is clear that size of stability region is very small in comparison to "*f*" family orbit [9]. So, these periodic orbits can be used as a transfer orbits as they are not stable. So, secondary body required few amount of fuel than Hohmann transfer. Figure 24 shows amplitude for two loop orbit when $q = 0.9845$. It can be observe that there are two separatrices at $C = 2.93$ and 2.95

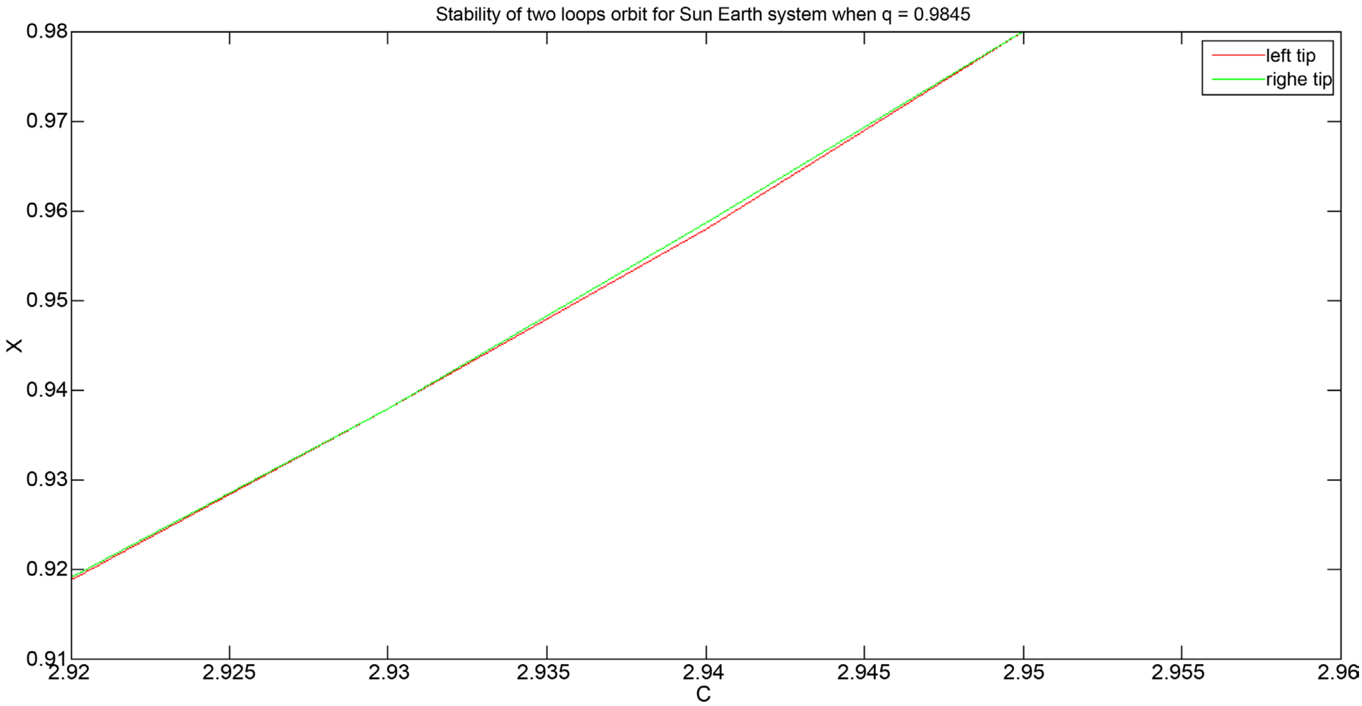

Figure 23. Stability analysis for two loops orbit for Sun-Earth system when $q = 0.9845$.

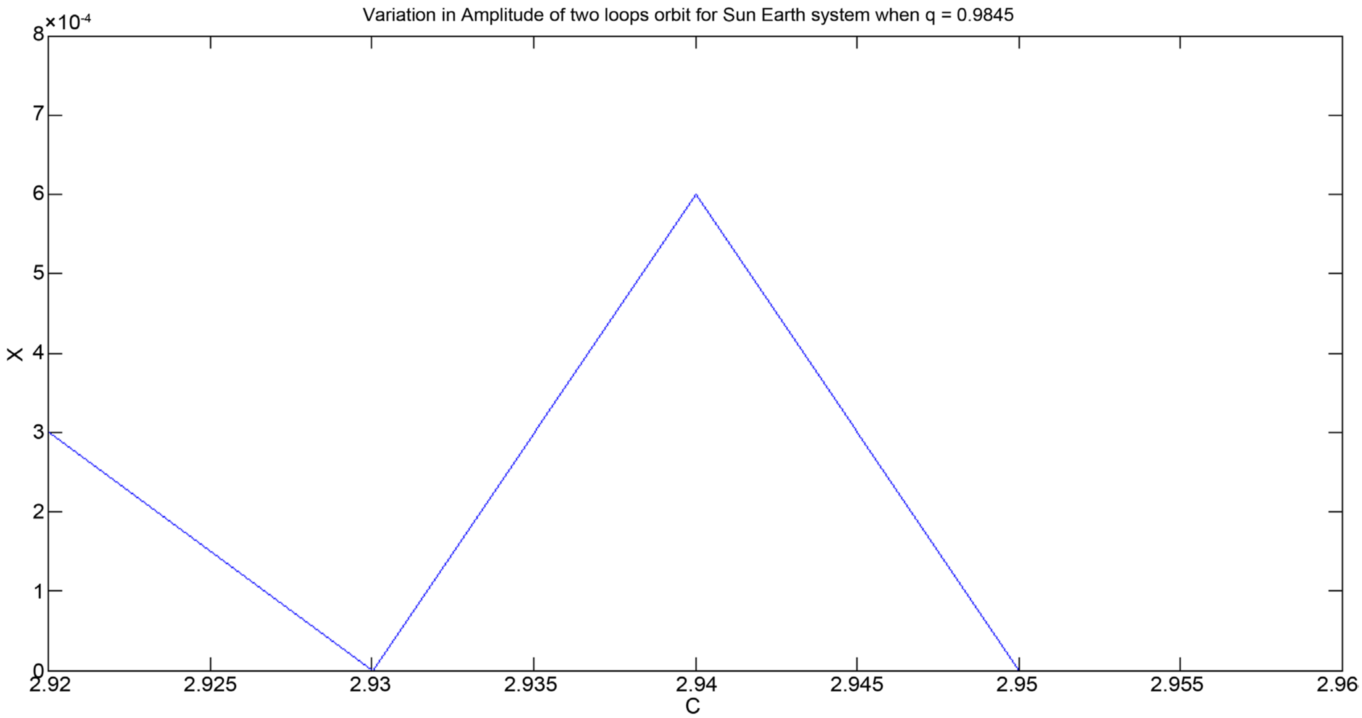

Figure 24. Amplitude for two loops orbit for Sun-Earth system when $q = 0.9845$.

where stability of the periodic orbit is zero as the size of the island is zero. For $C = 2.94$ we get maximum stability which is 0.0006. Figure 25 shows size of the island for $C = 2.92$ for two loop orbit when $q = 0.9845$ which is 0.0003 where as Figure 26 shows PSS

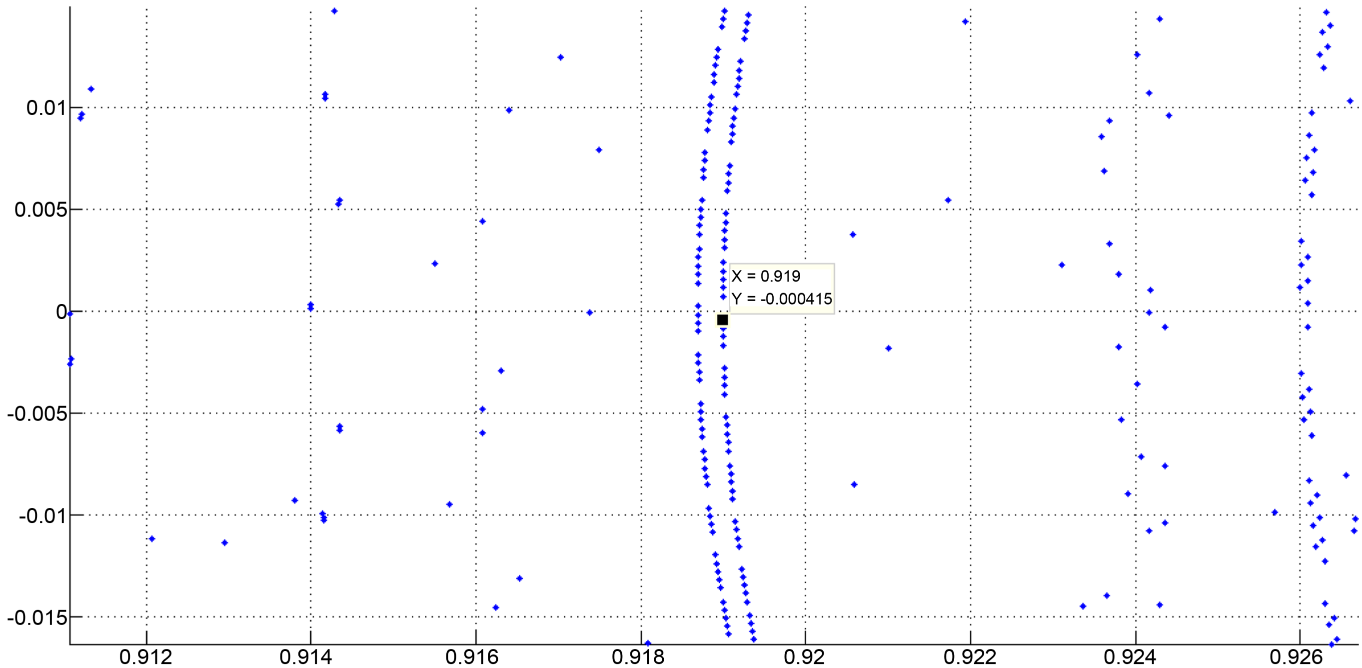

Figure 25. Enlarge view of PSS for $C = 2.92$ when $q = 0.9845$.

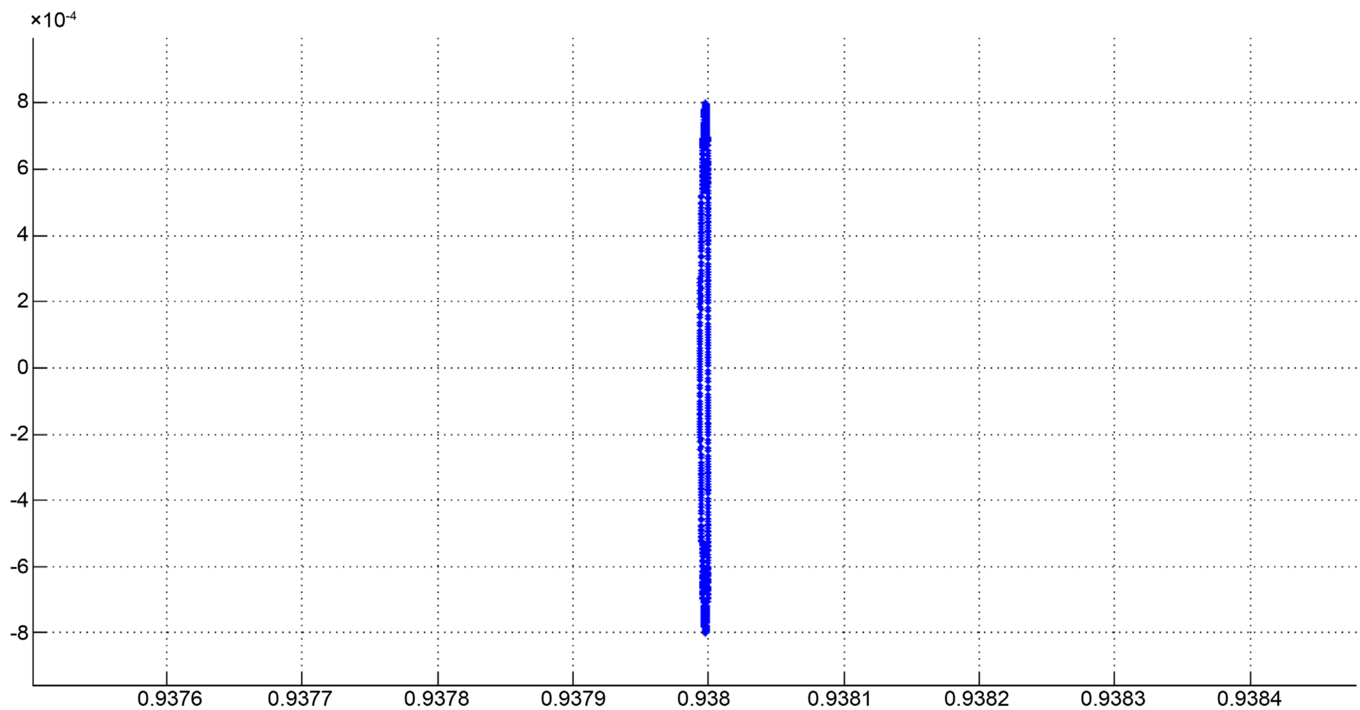

Figure 26. Enlarge view of PSS of first separatrix for two loop orbit for $C = 2.93$ when $q = 0.9845$.

of first separatrix at $C = 2.93$ which is looks like a straight line where as for "f" family orbit it is triangular due to third order resonance [9]. It can be seen that size of this island is zero. Figure 27 shows two loop orbit corresponding to first separatrix when $q = 0.9845$. Figure 28 shows for $C = 2.94$ again size of island increases and it becomes

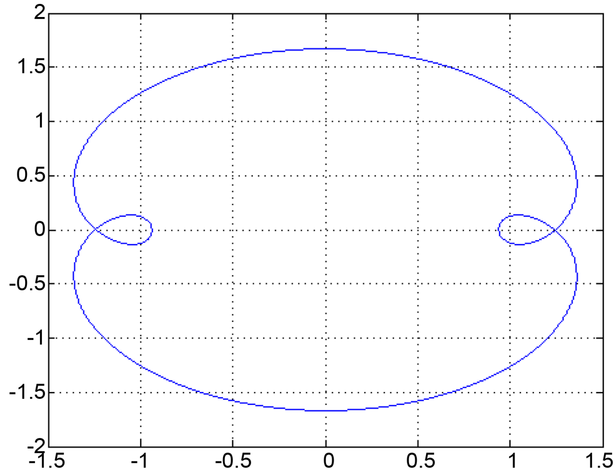

Figure 27. Orbit at first separatrix corresponding to C = 2.93, q = 0.9845 and x = 0.938.

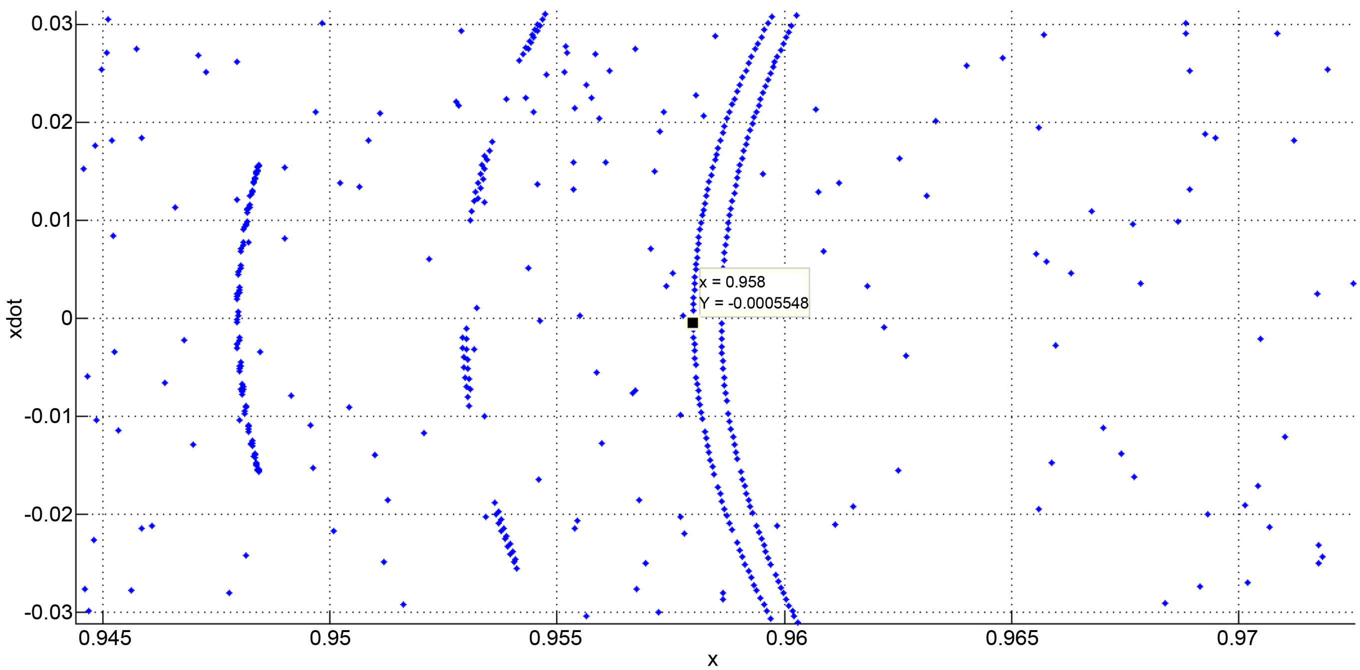

Figure 28. Enlarge view of PSS for C = 2.94 when q = 0.9845.

maximum, where as for C = 2.95 again size of island becomes zero, which is second separatrix as shown in **Figure 29**. Two loop orbit corresponding to second separatrix is given in **Figure 30**.

4. Conclusions

We have investigated the effect of solar radiation pressure on the position, shape and size of closed periodic orbit with loops varying from 1 to 5 for Sun-Mars and Sun-Earth systems, respectively. A noticeable difference observed in both the systems is that for C = 2.96, q = 0.995, single-loop periodic orbit, for C = 2.96, q = 0.99, two loops orbit, for C =

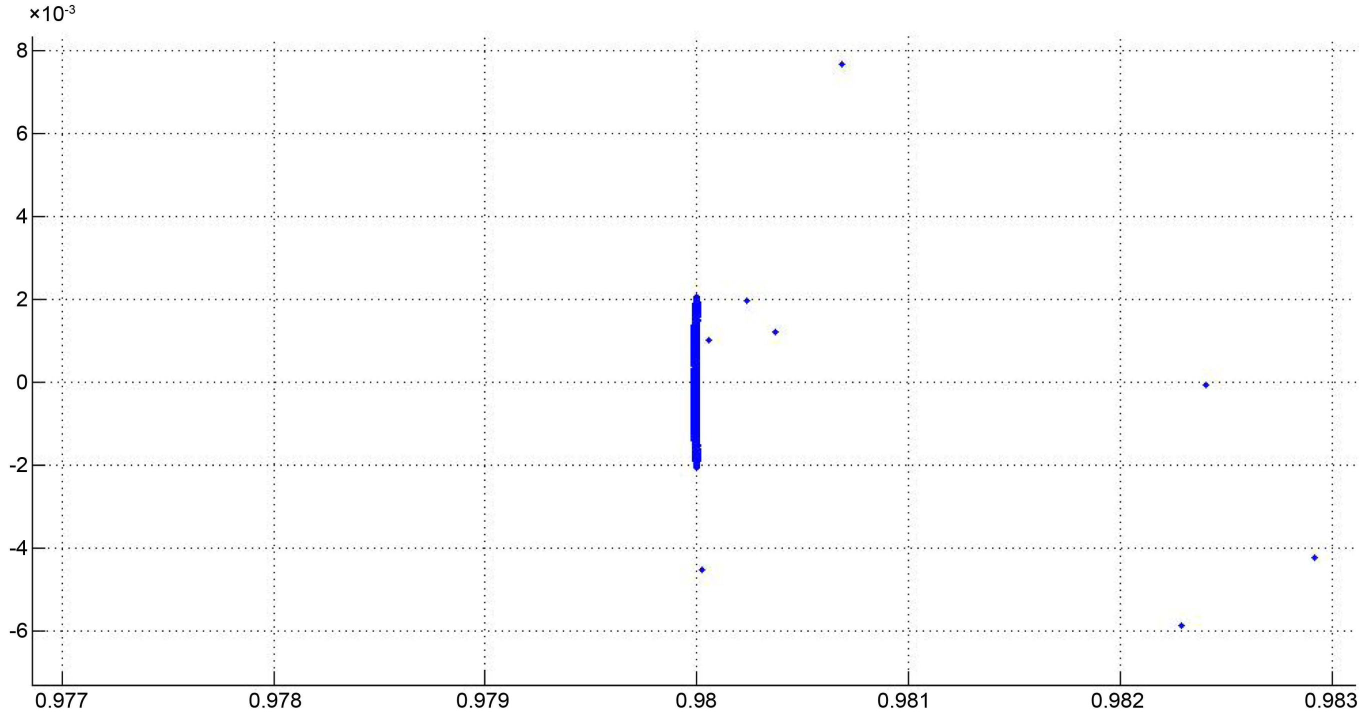

Figure 29. Enlarge view of PSS of second separatrix for two loop orbit for $C = 2.95$ when $q = 0.9845$.

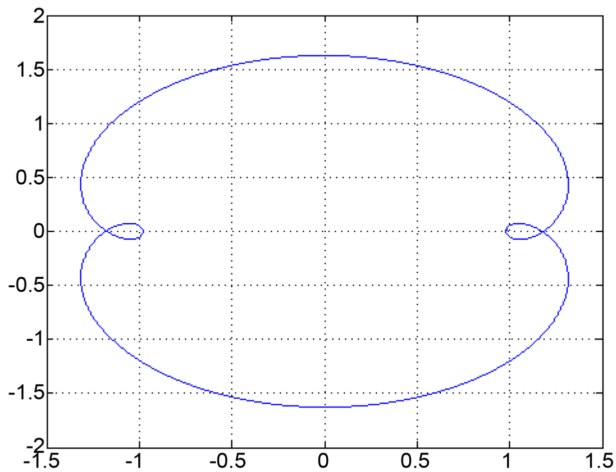

Figure 30. Orbit at second separatrix corresponding to $C = 2.95$, $q = 0.9845$ and $x = 0.98$.

2.96, $q = 0.9845$, three loops periodic orbit does not exist for Sun-Earth system whereas it exists for Sun-Mars system.

The distance of closest approach of the infinitesimal particle from the smaller primary decreases with increase in solar radiation pressure from 1 to 0.9845 and distance between smaller primary and infinitesimal particle increases as number of loops increases for a given C and q. It is found that the eccentricity decreases as number of loops increases. For a given number of loops, the eccentricity is found to decrease as solar radiation pressure increases from 1 to 0.9845. Thus, the present analysis of the two systems-Sun-Mars and Sun-Earth systems-using PSS technique reveals that q and C has substantial effect on the position, shape and size of the obit.

It can be observed that for given solar radiation pressure and given number of loops, as Jacobi constant decreases, initial velocity of infinitesimal particle (space craft) and distance of infinitesimal particle (space craft) from second primary increase and distance of infinitesimal particle (space craft) from first primary body decreases. For given Jacobi constant and given number of loops, as solar radiation pressure increases from 1 to 0.9845, initial velocity decreases and distance of infinitesimal particle (space craft) from second primary decreases. So, distance of infinitesimal particle (space craft) from first primary increases. Thus, the effect of Jacobi constant C and solar radiation pressure q is opposite in nature. For given value of solar radiation pressure q and Jacobi constant, as number of loops increases, distance of infinitesimal particle (space craft) from second primary increases and distance of infinitesimal particle (space craft) from first primary decreases. It is further observed that for Sun-Mars system, single loop orbit for q = 0.995 and C = 2.96 is closest to Mars and this distance is 7.521×10^5 km, whereas for Sun-Earth system, single loop orbit for q = 0.99 and C = 2.95 is closest to Earth and this distance is 7.535×10^5 km. Since these orbits can be used for designing low-energy space mission. Hence detailed study is presented in this paper.

Stability analysis of this family of orbit indicates that these orbits having smaller stability region in comparison to "*f*" family orbit. So, these orbits can be used as a transfer trajectory as less amount of fuel required for transferring of satellite from one orbit to another orbit. For each pair of (q, C), there are two separatrices exist where stability of periodic orbit becomes zero.

Acknowledgements

The authors thank Mrs. Pooja Dutt, Applied Mathematics Division, Vikram Sarabhai Space Centre (ISRO), Thiruvananthapuram, India for her constructive comments.

References

[1] Koon, W.S., *et al.* (2001) Low Energy Transfer to the Moon. *Celestial Mechanics and Dynamical Astronomy*, **81**, 63-73.

[2] Szebehely, V. (1967) Theory of Orbits. Academic Press, San Diego.

[3] Murray, C.D. and Dermot, S.F. (1999) Solar System Dynamics. Cambridge University Press, New York, USA.

[4] Dutt, P. and Sharma, R.K. (2010) Analysis of Periodic and Quasi-Periodic Orbits in the Earth-Moon System. *Journal of Guidance*, *Control*, *and Dynamics*, **33**, 1010-1017.

[5] Dutt, P. and Sharma, R.K. (2011) Evolution of Periodic Orbits in the Sun–Mars System. *Journal of Guidance*, *Control*, *and Dynamics*, **34**, 635-644.

[6] Safiyabeevi, A. and Sharma, R.K. (2011) Analysis of Periodic Orbits in the Saturn-Titan System Using the Method of Poincare Section Surfaces. *Astrophysics and Space Science*, **333**, 37-48.

[7] Dutt, P. and Sharma, R.K. (2012) On the Evolution of the "*f*" Family in the Restricted Three-Body Problem. *Astrophysics and Space Science*, **340**, 63-70.

[8] Pathak, N., Sharma, R.K. and Thomas, V.O. (2016) Evolution of Periodic Orbits in the Sun-Saturn System. *International Journal of Astronomy and Astrophysics*, **6**, 175-197.

[9] Pathak, N. and Thomas, V.O. (2016) Evolution of the "f" Family Orbits in the Photo Gravitational Sun-Saturn System with Oblateness. *International Journal of Astronomy and Astrophysics*, **9**, 254-271.

[10] Stromgren, E. (1935) O. Connaissance Actualle des Orbites dans le Problem des Trois Corps. Vol. 9, Publications and Minor Communications of Copenhagen Observatory, Publication 100, Copenhagen University, Astronomical Observatory, Denmark, 87.

[11] Sharma, R.K. (1987) The Linear Stability of Libration Points of the Photogravitational Restricted Three-Body Problem When the Smaller Primary Is an Oblate Spheroid. *Astrophysics and Space Science*, **135**, 271-281.

[12] Koon, W.S., *et al.* (2011) Dynamical Systems, the Three-Body Problem and Space Mission Design. http://www.cds.caltech.edu/~marsden/books/Mission_Design.html